A simplified characterization of *S*-adenosyl-L-methionine-consuming enzymes with 1-Step EZ-MTase: a universal and straightforward coupled-assay for *in vitro* and *in vivo* setting

Emmanuel S. Burgos*[a], Ryan O. Walters[b,c,d], Derek M. Huffman[b,c,d] and David Shechter*[a]

[a]*Department of Biochemistry, Albert Einstein College of Medicine, 1300 Morris Park Avenue, Bronx, New York 10461, United States*
Departments of [b]Molecular Pharmacology, [c]Medicine, and the [d]Institute for Aging Research, Albert Einstein College of Medicine, 1300 Morris Park Avenue, Bronx, New York 10461, United States

E-mail: emmanuel.burgos@einstein.yu.edu; Fax: +1-718-430-8565; Tel: +1-718-430-4128
E-mail: david.shechter@einstein.yu.edu; Fax: +1-718-430-8565; Tel : +1-718-430-4120

Electronic Supporting Information

Reagents and Analytical Procedures

Reagents−Common chemicals and reagents were obtained from commercial sources and used without further purification. D-luciferin (Gold Biolotechnology, #L-123), phosphoenolpyruvic acid (MP Biomedicals, #02151872), *S*-adenosyl-L-methionine (Sigma-Aldrich, #A7007; purification onto weak cation exchanger column –HiTrap CM Sepharose FF– is required to eliminate both *S*-adenosyl-L-homocysteine and 5′-deoxy-5′-methylthio-adenosine impurities),[1] 8-aza-adenosine (Berry & Associates, #PRA10007), sinefungin and sarcosine (Santa Cruz Biotechnology; #sc-203263 and #sc-204262, respectively).

HPLC methods−All purifications used a Luna C18(2) reversed phase column (Phenomenex #00G-4252-E0; 4.6 × 250 mm, 5 μm, 100 Å), with:

Buffer B1: 100 mM potassium dihydrogenophosphate with 8 mM tetrabutylammonium bisulfate in water (pH=6.00; KOH). Buffer B2: 100 mM potassium dihydrogenophosphate with 8 mM tetrabutylammonium bisulfate in 30% acetonitrile (pH=6.00; KOH).

Buffer B3: water. Buffer B4: 30% acetonitrile.

Buffer B5: 0.1% formic acid. Buffer B6: 0.1% formic acid in 50% acetonitrile.

Buffer B7: 100 mM acetic acid with 100 mM triethylamine (pH=6.00; formic acid). Buffer B8: 100 mM acetic acid with 100 mM triethylamine in 30% acetonitrile (pH=6.00; formic acid).

time	*flow*	**Method A**		**Method B**	
(min)	(mL min^{-1})	*B1*	*B2*	*B3*	*B4*
0	1	98	2	98	2
5	1	98	2	98	2
25	1	0	100	0	100
26	2	0	100	0	100
32	2	0	100	0	100
33	2	98	2	98	2
39	2	98	2	98	2
40	0	98	2	98	2

time	*flow*	**Method C**	
(min)	(mL min^{-1})	*B5*	*B6*
0	1	100	0
8	1	100	0
14	1	10	90
14.5	2	10	90
20.5	2	10	90
21	2	100	0
29	2	100	0
30	0	100	0

time	*flow*	**Method D**	
(min)	(mL min^{-1})	*B7*	*B8*
0	1	98	2
6	1	98	2
16	1	0	100
16.5	2	0	100
19.5	2	0	100
20	2	98	2
23	2	98	2
24	0	98	0

NMR spectroscopy−^{1}H (^{13}C) NMR spectra were recorded on a Bruker Avance IIIHD 600MHz (*150 MHz*) system equipped with a 5mm H/F-TCI CryoProbe. ICON-NMR software (Bruker Biospin) was used to record all spectra. The ^{1}H-^{1}H spectra were obtained at a constant temperature of 298 K using a COSY pulse sequence: 2048 and 128 points, sweep widths of 12 and offset 5.0 ppm in the primary and secondary direction, respectively and 4 scans. The ^{1}H-^{13}C *edited* spectra were obtained at a constant temperature of 298 K using the HSQC pulse sequence: with 2048 and 256 points, sweep widths of 12 and 200 ppm and offset 5.0 and 75 ppm for the ^{1}H and ^{13}C dimension, respectively and 16 scans. The length of standard proton pulse to achieve a 90° nutation was determined with the '*pulsecal*' command. The data were processed with Topspin

3.2 (Bruker Biospin) with baseline and phase correction. ^{31}P NMR spectra were recorded on a Bruker Avance IIIHD 300MHz (*121 MHz*) system equipped with a 5mm BBFO probe.

Mass spectrometry−Accurate mass measurements were performed using the Orbitrap Velos Mass Spectrometer (ThermoFisher) in the positive ionization mode at a resolution of 60,000 (at m/z 300) and using angiotensin as the lock mass. Flow injection analysis of 50% acetonitrile/water containing 0.1% formic acid was used to introduce the sample into the mass spectrometer at 0.075 mL min^{-1}. Prior to injection of 10 μL, 10 μL of a 10 μM solution of angiotensin in 50% acetonitrile/water containing 0.1% formic acid was mixed with 20 μL of a 50 μM solution of sample in water.

Enzymatic Syntheses

One-pot preparation of 8-aza-adenosine triphosphate (8-aza-ATP)−A 1.5-mL reaction mixture (100 mM TRIS/HEPES, 50 mM KCl, 40 mM $MgCl_2$, 2 mM βME, 450 mM phosphoenolpyruvate and 400 U pyruvate kinase/myokinase; pH=7.50) was carried out in a 2-mL tube containing 50 mg 8-aza-adenosine suspension (8-aza-A, C≈125 mM) and 1 mM ATP. Reaction started upon addition of adenosine kinase from *Anopheles gambiae* (*Ag*AK; 25 μM final concentration, enzyme:nucleoside is 1:5,000). Samples were mixed with a LabRoller™ rotator, and precipitate (8-aza-A) dissolved as mono-phosphorylation occurred within an hour. After 7 h (25 °C), reactions were stopped (Amicon Ultra-0.5 mL, MWCO 10K, 10,000 rpm; 4 °C, 15 min) and 8-aza-ATP (95% conversion) was isolated by HPLC (Method A−t_R(min): 8-aza-ATP 19.22, 8-aza-adenosine 12.77). The fraction containing 8-aza-ATP was freeze-dried and further desalting was performed (HPLC; Method B). A last lyophilization step offered pure 8-aza-ATP. ^{1}H NMR δ(600 MHz, D_2O) 4.17 (2 H, m, 5′-H), 4.43 (1 H, q, 4′-H, *J* 4.2), 4.76 (1 H, t, 3′-H, *J* 4.8), 5.16 (1 H, t, 2′-H, *J* 4.8), 6.34 (1 H, d, 1′-H, *J* 4.2), 8.36 (1 H, s, 2-H); ^{31}P NMR δ(121 MHz, D_2O) -23.13 (t, Pβ, *J* 19.7), -11.40 (d, Pα, *J* 19.6), -9.67 (br s, Pγ); ^{1}H−^{13}C *edited* HSQC NMR δ(150 MHz, D_2O) 65.2 (C-5′), 70.4 (C-3′), 73.2 (C-2′), 84.0 (C-4′), 88.2 (C-1′), 157.2 (C-2). FTMS + p ESI m/z 508.9981 (M^+), calcd for $[C_9H_{16}N_6O_{13}P_3]^+$ 508.9983.

Preparation of S-8-aza-adenosyl-L-methionine (8-aza-SAM)−A 1-mL reaction mixture (50 mM HEPES, 50 mM KCl, 10 mM $MgCl_2$, 1 mM βME, 25 mM phosphoenolpyruvate and 5 U pyruvate kinase/myokinase; pH=7.50) was carried out with 25 mM L-methionine and 10 mM of 8-aza-ATP. The synthesis started upon addition of methionine adenosyltransferase from *Methanococcus jannaschii* (*Mj*MAT; 25 μM final concentration, enzyme:triphosphate 1:400). After 2 h at 35 °C, reactions were stopped (Amicon Ultra-0.5 mL, MWCO 10K, 10,000 rpm; 4 °C, 15 min) and the SAM analog (65% conversion) was isolated by HPLC (Method C−t_R(min): 8-aza-SAM 4.67). The SAM analog-containing fraction was freeze-dried and further purified onto a weak cation exchanger column (HiTrap CM Sepharose FF, GE Healthcare Life Sciences, #17-5155-01; column was pre-charged with Na^+, impurities –including excess L-methionine– were eluted with water while 8-aza-SAM was stripped-off column with a 200 mM HCl solution). A final lyophilization step offered pure 8-aza-SAM as white powder. ^{1}H NMR δ(600 MHz, D_2O; *diluted sample*) 2.33 (2 H, m, β-H), 2.90 (3 H, s, S(*R*)Me; 5%), 2.94 (3 H, s, S(*S*)Me; 95%), 3.55 (2 H, m, 5′-H), 3.78 (1 H, m, α-H), 3.90 (2 H, m, γ-H), 4.66 (1 H, dd, 4′-H, J_a 6.6, J_b

5.4), 4.79 (1 H, m, 3′-H), 4.95 (1 H, dd, 2′-H, J_a 2.4, J_b 1.8), 6.47 (1 H, d, 1′-H, J 1.8), 8.39 (1 H, s, 2-H); ^{1}H−^{13}C *edited* HSQC NMR δ(150 MHz, D_2O; concentrated acidic sample) 23.6 (SMe), 24.7 (Cβ), 38.6 (C-5′), 44.6 (Cγ), 51.8 (Cα), 73.3 (C-3′), 73.9 (C-2′), 78.9 (C-4′), 90.3 (C-1′). FTMS + p ESI m/z 400.1398 (M^+), calcd for $[C_{14}H_{22}N_7O_5S]^+$ 400.1398.

Preparation of S-8-aza-adenosyl-L-homocysteine (8-aza-SAH)−The 7-mL reaction mixtures (100 mM TRIS, 100 μM $MgCl_2$, 1 mM βME, 10% glycerol; pH=7.90) were carried out with 40 mM sarcosine and 0.5 mM of 8-aza-SAM. The methyltransfer reactions started upon addition of *Gs*SDMT enzyme (10 μM final concentration; high excess to prevent product inhibition). After 1 h at 25 °C, reactions were stopped (Amicon Ultra-15 mL, MWCO 10K, 4,000 rpm; 4 °C, 20 min) and 8-aza-SAH (95% conversion) was isolated by HPLC (Method D−t_R(min): 8-aza-SAM 4.75, 8-aza-SAH 13.07). The 8-aza-SAH fractions were freeze-dried to offer white powder. ^{1}H NMR δ(600 MHz, D_2O) 2.02 (2 H, m, β-H), 2.60 (2 H, t, γ-H, J 7.8), 2.95 (2 H, dd, 5′-H, J_a 14.4, J_b 4.8), 3.74 (1 H, m, α-H), 4.39 (1 H, dd, 4′-H, J_a 7.2, J_b 4.8), 4.66 (1 H, t, 3′-H, J 4.8), 5.13 (1 H, dd, 2′-H, J_a 4.8, J_b 3.6), 6.35 (1 H, d, 1′-H, J 3.6), 8.35 (1 H, s, 2-H); ^{1}H−^{13}C *edited* HSQC NMR δ(150 MHz, D_2O) 27.6 (Cγ), 30.3 (Cβ), 33.4 (C-5′), 53.7 (Cα), 73.1 (C-3′), 73.6 (C-2′), 84.0 (C-4′), 88.7 (C-1′), 156.9 (C-2). FTMS + p ESI m/z 386.1233 (M^+), calcd for $[C_{13}H_{20}N_7O_5S]^+$ 386.1241 and 408.1058 (M-H+Na^+), calcd for $[C_{13}H_{19}N_7NaO_5S]^+$ 408.1061.

Preparation of S-8-aza-inosyl-L-homocysteine (8-aza-SIH)−The 1-mL reaction mixture (100 mM HEPES, 1 mM βME, 10% glycerol; pH=7.50) was carried out with 5 mM of 8-aza-SAH. The deaminase reaction started upon addition of TM0936 (50 μM final concentration). After 15 min at 35 °C, reaction was stopped (Amicon Ultra-0.5 mL, MWCO 10K, 10,000 rpm; 4 °C, 15 min) and 8-aza-SIH (100% conversion) was isolated by HPLC (Method D−t_R(min): 8-aza-SIH 11.60, 8-aza-SAH 13.07). The 8-aza-SIH fraction was freeze-dried to offer white powder. ^{1}H NMR δ(600 MHz, D_2O) 2.04 (2 H, m, β-H), 2.61 (2 H, t, γ-H, J 7.8), 2.96 (2 H, dd, 5′-H, J_a 14.4, J_b 4.8), 3.74 (1 H, m, α-H), 4.39 (1 H, dd, 4′-H, J_a 5.4, J_b 4.8), 4.65 (1 H, t, 3′-H, J 5.4), 5.10 (1 H, t, 2′-H, J 3.6), 6.37 (1 H, d, 1′-H, J 3.6), 8.33 (1 H, s, 2-H); ^{1}H−^{13}C *edited* HSQC NMR δ(150 MHz, D_2O) 27.5 (Cγ), 30.2 (Cβ), 33.4 (C-5′), 53.8 (Cα), 73.1 (C-3′), 73.7 (C-2′), 84.2 (C-4′), 89.1 (C-1′). FTMS + p ESI m/z 387.1081 (M^+), calcd for $[C_{13}H_{19}N_6O_6S]^+$ 387.1081 and 409.0897 (M-H+Na^+), calcd for $[C_{13}H_{18}N_6NaO_6S]^+$ 409.0901.

Purification of Enzymes

Photinus pyralis luciferase (FLUC)−The original wild-type firefly luciferase gene (pQE30-FLUC) was sub-cloned into the pMCSG10 vector to offer *N*-terminal His_6-GST-TEV-tagged enzyme.[2] BL21(DE3) cells, transformed with this new vector, were grown at 37 °C in LB broth containing 100 μg mL^{-1} ampicillin to an OD_{600}=0.6. The cultures were cooled down (18 °C), supplemented with IPTG (0.4 mM final concentration) and incubated for an additional 12 h. Harvested cells were re-suspended (50 mM TRIS, 300 mM NaCl, 5 mM imidazole, 1 mM βME, 10% glycerol, pH=8.00 containing PMSF and RNAse). Lysis was achieved using BugBuster® 10× and sonication; debris were removed by centrifugation at 20,000 rpm for 20 min. The supernatant was loaded onto Ni-NTA agarose and enzyme was eluted using an imidazole gradient (5−500 mM). Frac-

tions containing the tagged FLUC were concentrated, desalted, and further digested by His_6-tagged TEV protease (4 °C, 16 h). Subtractive Ni-NTA and further purification on Superdex 200 (16/300) column (50 mM TRIS, 300 mM NaCl, 1 mM βME, 10% glycerol, pH=8.00) offered FLUC. The concentrated enzyme (150 μM) was kept at -80 °C.

Proteins for enzymatic syntheses−For the synthesis of 8-aza-ATP and 8-aza-SAM, the *N*-terminal His_6-tagged adenosine kinase from *Anopheles gambiae* (*Ag*AK) and methionine adenosyltransferase from *Methanococus jannaschii* (*Mj*MAT) were expressed and purified as reported previously.[3-5] The sarcosine/dimethylglycine *N*-methyltransferase from *Galdieria sulphuraria* (*Gs*SDMT; DNASU clone ID GsCD00383580) was used for the preparation of 8-aza-SAH, by-products of this methyltransferase reaction with sarcosine and corresponding 8-aza-SAM.[6]

Methyltransferases−The PRMT5 from *Caenorhabditis elegans* (*Ce*PRMT5) was expressed and purified as described previously with some modification.[7,8] In addition to Triton X-100 (1%), prior use of BugBuster® reagent for cell lysis also improved yield of recovered protein. The PRMT7 from *Trypanosoma brucei* (*Tb*PRMT7) was prepared using a published protocol.[9] The $H4_{(1-20)}$ peptide substrate for *Ce*PRMT and *Tb*PRMT7 was purchased from GenScript (>95%). Following the described procedures, the histone H3 Lysine-K9 methyltransferase from *Neurospora crassa* (*Nc*DIM-5) was expressed and purified as a GST-tagged enzyme.[10] The $H3_{(1-53)}$ peptide substrate for DIM-5 was expressed as a His_6-tagged peptide from a modification of the original vector with a stop codon (Y54Stop).[11] Ni-NTA purification, followed by removal of *N*-terminus tag with His_6-TEV protease (4 °C, 16 h) and subtractive Ni-NTA offered $H3_{(1-53)}$. Peptide was purified by HPLC,[11] and further lyophilization offered suitable substrate for DIM-5 kinetic studies. The sarcosine/dimethylglycine *N*-methyltransferase from *Galdieria sulphuraria* (*Gs*SDMT; DNASU clone ID GsCD00383580) was expressed as a His_8-MBP-tagged enzyme (maltose binding protein). Further removal of the His_8-MBP-tag with His_6-tagged TEC protease (4 °C, 16 h) and gel filtration step offered purified enzyme.[6] The human glycine *N*-methyltransferase (*Hs*GNMT) was expressed as a tag-less enzyme in *E. coli*; sequential purification by ammonium sulfate fractionation, ion-exchange chromatography and gel-filtration was performed as previously described.[12]

TM0936 coupling enzyme−The SAH-deaminase from *Thermotoga maritima* (gene TM0936; DNASU clone ID TmCD00084735) was expressed and purified as described in a previous report.[13] Likewise, the preparation of 5′-methylthioadenosine/*S*-adenosyl-L-homocysteine nucleosidase from *Salmonella enterica* (*Se*MTAN) was previously reported.[14]

pH-, Salt- and DMSO-dependence of FLUC Luminescence

Relative enzymatic efficiency of FLUC upon pH variation−The impact of pH onto enzymatic efficiency for recombinant FLUC was determined at 25 °C by monitoring luminescence (RLU, relative light unit) with a SpectraMax L instrument (one photomultiplier, 'photo-counting' mode; Molecular Devices). Briefly, 90-μL reactions containing buffer (50 mM phosphate; pH 5.80−8.00), 1 mM $MgCl_2$, 1 mM βME, 10% glycerol, 10 μM of both ATP and luciferin, were loaded onto a 96-well half-area flat bottom plate (Corning, #3992). Light production started upon addition of FLUC recombinant enzyme (10 μL at

10 nM) and RLU were recorded. For optimum experimental condition (*i.e.* pH=8.00), the RLU was set to 1.0 and corresponding ratios were determined for other experiments.

Salt and DMSO effect on FLUC luminescence−Using the same experimental procedure as above (50 mM phosphate, pH=8.00), luminescence was recorded under various concentrations of either NaCl (0−500 mM) or DMSO (0−7.5%, v/v). Light production started upon addition of FLUC recombinant enzyme (10 μL at 10 nM) and RLU were monitored. For optimum experimental condition (*i.e.* no salt, no DMSO), the RLU was set to 1.0 and corresponding ratios were determined for other experiments.

Spectral analysis of the FLUC luminescence−The spectral components of FLUC luminescence were observed at various pHs (50 mM phosphate buffer) by mixing ATP (1 mM), luciferin (1 mM), $MgCl_2$ (5 mM), 1 mM βME, 10% glycerol and FLUC (1 μM) in a 96-well half-area flat bottom plate. Lower pH values drastically affect the enzyme and shift its luminescence towards a red emission spectrum, with light production no longer occurring below pH=6.00. A semi-quantitative analysis of the FLUC luminescence (pHs 8.00, 7.20 and 6.40) was performed under the same conditions using a quartz cuvette and a FluoroMax-3 fluorometer (3-mL reaction volume; emission scan: 450−750 nm, 5 nm s^{-1}; excitation slit width 'shutoff', emission slit width 10 nm). The light generated upon luciferin oxidation was a combination of three spectral components with maximum emission at 556, 606 and 654 nm; thus, experimental traces RLU = f(λ) were fitted to a three-component Gaussian function (supplementary Eq. S1):[15]

$$RLU = RLU_{556}^{MAX} e^{-0.5\left(\frac{\lambda-556}{\sigma_{556}}\right)^2} + RLU_{606}^{MAX} e^{-0.5\left(\frac{\lambda-606}{\sigma_{606}}\right)^2} + RLU_{654}^{MAX} e^{-0.5\left(\frac{\lambda-654}{\sigma_{654}}\right)^2} \quad \textbf{(S1)}$$

where λ is the scanned emission wavelength (FLUC), RLU^{MAX} and σ are the luminescence intensity and the Gaussian RMS width at the specific maximum emission wavelength (*i.e.* 556, 606 or 654 nm), respectively.

Differential Extinction Coefficients (*Δε*) for Deaminase Reaction

Nucleoside concentrations (stock solutions) were determined using known extinction coefficients for: adenosine, 259(ε/M^{-1} cm^{-1} 15,400) and 8-aza-adenosine, 277(ε/M^{-1} cm^{-1} 17,830). The deaminase reactions using these various substrates were performed in quartz cuvettes (1-cm light path; 3-mL reaction volume) and absorbance measurements were carried out with a NanoDrop 2000c (scan mode: 220−320 nm with multi scans superimposed; 37 °C and continuous stirring). Briefly, the 3-mL reactions contained 50 mM buffer (acetate: pH 4.00−5.00; MES: pH 5.00−6.50; phosphate: pH 5.80−8.00; TRIS: pH 7.50−8.50; CHES: pH 8.90−9.90), 1 mM βME and 10% glycerol. Five different concentrations of either adenosine or 8-aza-adenosine substrates were used (10, 20, 30, 40 and 50 μM). Mixtures were blanked before acquisition and reactions started upon addition of deaminase (TM0936, 2 μL of 240.5 μM enzyme stock). Over the course of the deaminase reaction (*e.g.* adenosine → inosine), optimum wavelengths at which the highest absorbance shift is observed were selected (*i.e.* adenosine reaction, λ=263 nm; 8-aza-adenosine reaction, λ1=282 nm and λ2=292 nm). Scans were recorded until the absorbance at these monitored wavelengths reached a stable value.[16] For each pH condition, the end-point absorbance shifts were plotted against initial nucleoside con-

centrations and fitted to a linear regression: each slope is a differential extinction coefficient ($\Delta\varepsilon$) for deamination of the specific nucleoside substrate. Furthermore, the pH-dependence of differential extinction coefficient ($\Delta\varepsilon$) for this deaminase reaction was obtained by plotting the pairs ($\Delta\varepsilon$; pH) and fitting these to the following supplementary Eq. S2:

$$\Delta\varepsilon = \Delta\varepsilon_{HIGH\ pH} + \frac{\Delta\varepsilon_{LOW\ pH} - \Delta\varepsilon_{HIGH\ pH}}{1 + 10^{(pH - pK_a)}} \quad \textbf{(S2)}$$

where $\Delta\varepsilon_{\text{HIGH pH}}$ and $\Delta\varepsilon_{\text{LOW pH}}$ are the extinction coefficient measured at optimum wavelengths (*i.e.* λ for adenosine and λ1 or λ2 for 8-aza-adenosine) for the deaminase reaction at high and low pH, respectively, and -pKa is the logarithm of acid dissociation constant for either inosine or 8-aza-inosine. In summary: adenosine → inosine, 263($\Delta\varepsilon_{\text{HIGH pH}}$; $\Delta\varepsilon_{\text{LOW pH}}$/$M^{-1}$ cm^{-1} -4,655 ± 186; -8,076 ± 80), pK_a=8.72 ± 0.09; 8-aza-adenosine → 8-aza-inosine, 282($\Delta\varepsilon_{\text{HIGH pH}}$; $\Delta\varepsilon_{\text{LOW pH}}$/$M^{-1}$ cm^{-1} -2,026 ± 174; -14,975 ± 129), pK_a=7.29 ± 0.03, 292($\Delta\varepsilon_{\text{HIGH pH}}$; $\Delta\varepsilon_{\text{LOW pH}}$/$M^{-1}$ cm^{-1} -3,016 ± 119; -10,117 ± 87), pK_a=7.30 ± 0.03.

Dynamic range of the SAH-detection and Z′-factor

Upper and lower limit of the SAH-detection−To establish the upper limit of SAH-detection, increasing concentrations of *Gs*SDMT (0−3.66 μM) were used to methylate sarcosine (10 mM) in the presence of a saturating concentration of SAM (770 μM) at pH 7.80 (100 mM phosphate, 5% glycerol, 0.1 mM $MgCl_2$, 1 mM βME, 4 μM TM0936). Methyltransfer rates were recorded in a 96-well plate (60 μL) following loss of absorbance at 263 nm. The initial rates for sarcosine methylation were plotted against *Gs*SDMT concentrations. The relationship between these two parameters is linear below the upper limit of SAH-detection (Rmax). Above Rmax, the deamination catalyzed by TM0936 is rate limiting and the loss of absorbance at 263 nm does not accurately report on the methyltransfer. Likewise, to determine the lower limit of SAH-detection, decreasing concentrations of *Nc*DIM-5 (17.45−0 nM) were used to methylate $H3_{(1-53)}$ peptide (25 μM) in the presence of a saturating concentration of SAM (25 μM) at pH 9.50 (25 mM glycine, 10% glycerol, 1 mM βME, 50 mM NaCl, 4 μM TM0936). Methyltransfer rates were recorded in a 96-well plate (250 μL) following loss of absorbance at 263 nm. The initial rates for $H3_{(1-53)}$ methylation were plotted against *Nc*DIM-5 concentrations. Although the relationship between these two parameters is linear across the whole range of methyltransferase concentrations, a lower limit of SAH-detection (Rmin) is established above the background signal. SAM cofactor is unstable and slowly decomposes into SAH, further deaminated by TM0936. Below Rmin, the discrimination between methyltransfer and natural decomposition of SAM is inaccurate.

Z′-factor−The screening window coefficient (*Z′*-factor) was determined as previously described using various *Ce*PRMT5, *Tb*PRMT7, *Nc*DIM-5 and *Gs*SDMT enzyme concentrations (116−1000 nM, 139−1003 nM, 4.28−23.8 nM and 19.5−244 nM, respectively) with saturating concentrations of SAM (25.0, 25.1, 25.8 and 763 μM, respectively) and saturated levels of matching acceptor (acceptor/μM: $H4_{(1-20)}$/200, $H4_{(1-20)}$/200, $H3_{(1-53)}$/15.8 and sarcosine/5,000, respectively) at either pH=7.60 (50 mM phosphate), pH=7.60 (50 mM phosphate), pH=9.50 (50 mM glycine) or pH=7.80 (50 mM phosphate),

respectively.[17] Each experiment consisted of 8 sample replicates (*s*; with both SAM and acceptor included in reactions) and 8 control replicates (*c*; with SAM and without acceptor in reactions). Statistical analysis of the initial rates using the following supplementary Eq. S3 yields the corresponding Z′-factor:

$$Z' = 1 - \frac{3\sigma_s + 3\sigma_c}{|\mu_s - \mu_c|} \quad \textbf{(S3)}$$

where μ_s is the mean value of the initial rates for samples *s* and σ_s is the standard deviation of the initial rates for samples *s* ($3\sigma_s$ corresponds to a 99.73% confidence interval).

UV-based Coupled Assay for MTases

The Excel files "*My 1-Step EZ-MTase Assay (UV) Acceptor Km.xlsx*" and "*My 1-Step EZ-MTase Assay (UV) CoFactor Km.xlsx*" (*cf*. ESI) provide two exhaustive templates to help the users in 1) setting-up their experimental conditions (worksheet "*Experiment Conditions*"), 2) importing their raw data (worksheet "*Plate Reader Data*"), 3) reporting their key experimental conditions (*e.g.* pH, nature of methyl cofactor being used; worksheet "*Coupling Enzyme Parameters*" and 4) computing and displaying the kinetic parameters of their very own experiment.

Kinetic behavior for peptide H4$_{(1-20)}$ against CePRMT5 (SAM sat.)−Briefly, kinetic parameters were determined at 20 °C in a UV-Star 96-well flat bottom plate (Greiner Bio-One, #655801) by continuous monitoring of absorbance at 263 nm using a SpectraMax M5 instrument (Molecular Devices). The 250-μL reaction mixtures from a same row contained 50 mM phosphate buffer pH=7.60, 1 mM βME, 10% glycerol, 4 μM coupling deaminase TM0936, 300 nM *Ce*PRMT5 and various peptide concentrations (5−180 μM; in the first well, peptide acceptor was omitted to account for background signal −natural decomposition of SAM). The methyltransfer reactions started upon addition of SAM (25 μM saturating final concentration) and absorbance was recorded. Initial rates were first corrected for background signal, then plotted against H4$_{(1-20)}$ concentrations and fitted to the Morrison kinetic model (supplementary Eq. S4) to yield corresponding kinetic parameters (K_m, k_{cat}):[18]

$$v = 0.5\, k_{cat}\left(([MTase] + [H4] + K_m) - \sqrt{([MTase] + [H4] + K_m)^2 - 4[MTase][H4]}\right) \quad \textbf{(S4)}$$

where [MTase] and [H4] are the total concentration of methyltransferase and peptide acceptor, respectively; K_m is the Michaelis constant and k_{cat} is the turnover for H4$_{(1-20)}$ substrate.

Kinetic behavior for SAM against CePRMT5 (H4$_{(1-20)}$ sat.)−Briefly, the measurements consisted of two experimental subsets: MTase reactions (both SAM and peptide added) and MTase blanks (SAM was added without peptide to account for natural SAM decomposition). The 250-μL reaction mixtures from a same row contained 50 mM phosphate buffer pH=7.60, 1 mM βME, 10% glycerol, 4 μM coupling deaminase TM0936, 300 nM *Ce*PRMT5 and various SAM concentrations (2.35−47.0 μM). Absorbance at 263 nm was recorded after addition of either H4$_{(1-20)}$ (104 μM saturating final concentra-

tion; MTase reactions) or water (MTase blanks). Initial rates were first corrected for background signal, then plotted against SAM concentrations and fitted to the Morrison kinetic model to yield corresponding kinetic parameters.

Kinetic behavior for peptide H4$_{(1-20)}$ against TbPRMT7 (SAM sat.)−Experiments were conducted following the matching *Ce*PRMT5 protocol above. Briefly, the 250-μL reaction mixtures from a same row contained 25 mM phosphate buffer pH=7.60, 1 mM βME, 10% glycerol, 4 μM coupling deaminase TM0936, 1.0 μM *Tb*PRMT7 and various peptide concentrations (16.6−243.3 μM; in the first well, peptide acceptor was omitted to account for background signal −natural decomposition of SAM). Reactions started upon addition of SAM (25.8 μM saturating final concentration) and absorbance was recorded. Initial rates were first corrected for background signal, then plotted against H4$_{(1-20)}$ concentrations. Fit to the Michaelis-Menten model (supplementary Eq. S5) provided corresponding kinetic parameters:

$$v = k_{cat}\frac{[MTase][H4]}{K_m + [H4]} \quad \textbf{(S5)}$$

where [MTase] and [H4] are the total concentration of methyltransferase and H4 peptide, respectively; K_m is the Michaelis constant and k_{cat} is the turnover for H4 substrate.

Kinetic behavior for SAM against TbPRMT7 (H4$_{(1-20)}$ sat.)−Experiments were conducted following the matching *Ce*PRMT5 protocol above. Briefly, the measurements consisted of two experimental subsets: MTase reactions (both SAM and peptide added) and MTase blanks (SAM was added without peptide to account for natural SAM decomposition). The 250-μL reaction mixtures from a same row contained 25 mM phosphate buffer pH=7.60, 1 mM βME, 10% glycerol, 4 μM coupling deaminase TM0936, 402 nM *Tb*PRMT7 and various SAM concentrations (1.53−20.0 μM). Absorbance at 263 nm was recorded after addition of either H4$_{(1-20)}$ (200 μM saturating final concentration; MTase reactions) or water (MTase blanks). Initial rates were first corrected for background signal, then plotted against SAM concentrations and fitted to the Morrison kinetic model to yield corresponding kinetic parameters.

Kinetic behavior for peptide H3$_{(1-53)}$ against NcDIM-5 (SAM sat.)−Experiments were conducted following the matching *Ce*PRMT5 protocol above. Briefly, the 250-μL reaction mixtures from a same row contained 25 mM glycine buffer pH=9.50, 1 mM βME, 10% glycerol, 50 mM NaCl, 4 μM coupling deaminase TM0936, 7.6 nM *Nc*DIM-5 and various peptide concentrations (0.51−12.68 μM; in the first well, peptide acceptor was omitted to account for background signal −natural decomposition of SAM). Reactions started upon addition of SAM (25.8 μM saturating final concentration) and absorbance was recorded. Initial rates were first corrected for background signal, then plotted against H3$_{(1-53)}$ concentrations. Fit to the Michaelis-Menten equation provided corresponding kinetic parameters.

Kinetic behavior for sarcosine against GsSDMT (SAM sat.)−Experiments were conducted following matching *Ce*PRMT5 protocol above. Briefly, the 100-μL mixtures from a same row contained 100 mM phosphate buffer pH=7.80, 1 mM βME, 5% glycerol, 100

μM $MgCl_2$, 4 μM coupling deaminase TM0936, 976 nM *Gs*SDMT and various sarcosine concentrations (0.5−12.5 mM; sarcosine was omitted in the first well to account for background signal −natural decomposition of SAM). Reactions started upon addition of SAM (750 μM saturating final concentration), and 60-μL volumes were transferred onto UV-plate and absorbance was read at 263 nm. Initial rates were first corrected for background signal, and then plotted against sarcosine concentrations. Fit to the Michaelis-Menten equation provided corresponding kinetic parameters.

Kinetic behavior for SAM against GsSDMT (sarcosine sat.)−Experiments were conducted following matching *Ce*PRMT5 protocol above. Briefly, the measurements consisted of two experimental subsets: MTase reactions (both SAM and sarcosine added) and MTase blanks (SAM was added without sarcosine to account for natural SAM decomposition). The 100-μL reaction mixtures from a same row contained 100 mM phosphate buffer pH=7.80, 1 mM βME, 5% glycerol, 100 μM $MgCl_2$, 4 μM coupling deaminase TM0936, 195 nM *Gs*SDMT and various SAM concentrations (49.9−750.2 μM). Reactions started upon addition of either sarcosine (10 mM saturating final concentration; MTase reactions) or water (MTase blanks), 60-μL volumes were transferred onto UV-plate and absorbance was recorded at 263 nm. Initial rates were first corrected for background signal, and then plotted against SAM concentrations. Fit to the Michaelis-Menten equation provided corresponding kinetic parameters.

Kinetic behavior for 8-aza-SAM against MTases (acceptor sat.)−Briefly, kinetic parameters were determined at 20 °C in a UV-Star 96-well flat bottom plate (Greiner Bio-One, #655801) by continuous monitoring of absorbance at 282 nm using a SpectraMax M5 instrument (Molecular Devices). As for SAM experiments, the measurements consisted of two experimental subsets: MTase reactions (both 8-aza-SAM and acceptor added) and MTase blanks (8-aza-SAM was added without acceptor to account for natural 8-aza-SAM decomposition). The 250-μL (60-μL) reaction mixtures from a same row contained 50 mM phosphate buffer pH=7.60 (7.80), 1 mM βME, 10% glycerol (5% glycerol, 100 μM $MgCl_2$), 4 μM coupling deaminase TM0936, either 1.5 μM *Ce*PRMT5 or 402 nM *Tb*PRMT7 (or 610 nM *Gs*SDMT) and various 8-aza-SAM concentrations. Absorbance at 282 nm was recorded after addition of either $H4_{(1\text{-}20)}$ (104 μM saturating final concentration; MTase reactions) or water (MTase blanks) (of either sarcosine (5 mM saturating final concentration; MTase reactions) or water (MTase blanks)). Initial rates were first corrected for background signal, then plotted against 8-aza-SAM concentrations and fitted to the Michaelis-Menten equation to yield corresponding kinetic parameters. The kinetic data from *Ce*PRMT5 were fit to the following supplementary Eq. S6 to reflect substrate inhibition observed at higher 8-aza-SAM concentration:

$$v = \frac{k_{cat}[MTase][8-aza-SAM]}{K_m + [8-aza-SAM] + \frac{[8-aza-SAM]^2}{K_s}} \quad \textbf{(S6)}$$

where [MTase] and [8-aza-SAM] are the total concentration of methyltransferase and methyl donor, respectively. K_m is the Michaelis constant, K_s is the substrate inhibition constant and k_{cat} is the turnover for 8-aza-SAM substrate. Please note that DIM-5 was unable to accept 8-aza-SAM substrate.

Study of *Gs*SDMT inhibition by sinefungin (UV-mode)

The Excel file "*My 1-Step EZ-MTase Assay (UV) SIN Ki.xlsx*" (*cf*. ESI) provides an exhaustive template to assist users with the procedure. Briefly, kinetic parameters were determined at 20 °C in a UV-Star 96-well flat bottom plate (Greiner Bio-One, #655801) by continuous monitoring of absorbance at 263 nm using a SpectraMax M5 instrument (Molecular Devices). The 100-μL reaction mixtures from a set of two rows contained 100 mM phosphate buffer pH=6.80, 1 mM βME, 5% glycerol, 100 μM $MgCl_2$, 4 μM coupling deaminase TM0936, 195 nM *Gs*SDMT, saturating level of SAM (763 μM) and various sinefungin concentrations (0.8−244 μM). In the first row, the sarcosine acceptor was omitted to account for background signal (*i.e.* natural catabolism of sinefungin and SAM decomposition). The methyltransfer reactions started upon addition of sarcosine (5 mM saturating final concentration). Volumes (60-μL) were transferred onto plate and absorbance signals were recorded. The initial rates of the reactions were corrected using data from first row experiments and plotted against sinefungin concentrations. Fit to the following supplementary Eq. S7 provided corresponding inhibition constant (K_i):

$$V/V_0 = \frac{K_m + [SAM]}{K_m + [SAM] + \left(K_m \left(\frac{10^{Log[SIN]}}{K_i}\right)^{\gamma}\right)} \quad \textbf{(S7)}$$

where V and V_0 are the initial velocity with and without inhibitor, respectively. The Michelis constant for SAM substrate is depicted as K_m and [SAM] is the concentration of this same molecule. The inhibition constant for sinefungin is represented by K_i and [SIN] is the concentration of this inhibitor. The parameter γ is the Hill coefficient.

The k_{cat} and k_{cat}/K_m pH-dependence for the *Gs*SDMT reaction

Experiments were conducted following *Gs*SDMT protocol above using 100 mM buffer (pH 5.80−9.88), 1 mM βME, 5% glycerol, 100 μM $MgCl_2$, 4 μM coupling deaminase TM0936, 976 nM *Gs*SDMT and various sarcosine concentrations (0.5−12.5 mM; in the first well, sarcosine was omitted to account for background signal −natural decomposition of SAM). Reactions started upon addition of SAM (750 μM saturating final concentration) and 60-μL volumes were transferred onto UV-plate. Absorbance at 263 nm was recorded. After correction for background signal, initial velocities were plotted against sarcosine concentrations. Fit to the Michaelis-Menten equation provided corresponding K_m and k_{cat}. Both kinetic parameters were used to plot the corresponding pH-dependences using the two following supplementary Eq. S8 and S9:[19]

$$log\left(\frac{k_{cat}}{K_m}\right) = log(V_{max}^{MAX}) - log\left(\left(1 + \frac{10^{-pH}}{10^{-pK_a^1}} + \frac{10^{-pK_a^2}}{10^{-pH}}\right)^2\right) \quad \textbf{(S8)}$$

where K_m and k_{cat} are the Michaelis constant and turnover value, respectively, for sarcosine substrate at saturating levels of SAM (750 μM). V_{max}^{MAX} is the maximum velocity ever achieved by the *Gs*SDMT enzyme over the full pH-range. The -pK_a^1 and -pK_a^2 are

the logarithm of acid dissociation constant for a first and a second ionizable group of important entities: these entities are free sarcosine and *Gs*SDMT•SAM complex.

$$log(k_{cat}) = log(k_{cat}^{MAX}) - log\left(1 + \frac{10^{-pH}}{10^{-pK_a^1}}\right) \quad \textbf{(S9)}$$

where k_{cat} is turnover value for sarcosine substrate at saturating levels of SAM (750 μM); k_{cat}^{MAX} is maximum turnover value for sarcosine substrate ever reached; the parameter -pK_a^1 is the logarithm of the acid dissociation constant from a crucial ionizable group onto the *Gs*SDMT•SAM•sarcosine complex.

Impact of ionic strength onto K_m for H4$_{(1-20)}$ (*Tb*PRMT7)

Experiments were conducted following the *Tb*PRMT7 protocol above. Briefly, the 250-μL reaction mixtures from a same row contained either 25, 50, 75 or 100 mM phosphate buffer pH=7.60, 1 mM βME, 10% glycerol, 4 μM coupling deaminase TM0936, 1.0 μM *Tb*PRMT7 and various peptide concentrations (16.6−243.3 μM; in the first well, peptide acceptor was omitted to account for background signal −natural decomposition of SAM). Reactions started upon addition of SAM (25.8 μM saturating final concentration) and absorbance was recorded. Initial rates were first corrected for background signal, then plotted against H4$_{(1-20)}$ concentrations. The four fits to the Michaelis-Menten equation (k_{cat} fixed at 29 h^{-1}) provided corresponding K_m values and established impact of ionic strength onto this kinetic parameter.

Fluorescence-based coupled assay

Calibration of fluorescence signal for the 8-aza-A to 8-aza-I reaction−This procedure is very similar to the one described under "**Differential Extinction Coefficients (Δε) for Deaminase Reaction**". Briefly, standard solutions (240 μL) of 8-aza-adenosine (0−25 μM; 12 data points) containing 50 mM buffer (pH 5.00−9.50), 10% glycerol and 1 mM βME, were loaded into a 96-well black flat bottom plate. 10-μL water per well were added to one data-set (12 concentrations of 8-aza-adensoine); 10-μL TM0936 solution (24.05 μM) were added to the remaining samples (12 concentrations of 8-aza-adenosine at various pH values). The loss of fluorescence (*Em*=360 nm) from 8-aza-adenosine standard solutions (*Ex*=282/292 nm) where recorded with a Spectramax M5 plate reader until no change in signal could be observed.

The comparison between end-point deaminase reactions and reference well at the same pH (TM0936 added but no 8-aza-adenosine) provided the pH-dependence of 8-aza-inosyl fluorescence. Using the *Ex/Em* pair (282/360 nm), the data fit to the supplementary Eq. S2 provided the following parameters: $FLUO_{LOW\ pH}$ = 0 RLU μM^{-1}, $FLUO_{HIGH\ pH}$ = 35.0 ± 0.5 RLU μM^{-1}, pK_a = 7.50 ± 0.03. Likewise, using the *Ex/Em* pair (292/360 nm), the data fit to the supplementary Eq. S2 provided the following parameters: $FLUO_{LOW\ pH}$ = 1.5 ± 0.3 RLU μM^{-1}, $FLUO_{HIGH\ pH}$ = 22.0 ± 0.3 RLU μM^{-1}, pK_a = 7.54 ± 0.04. Furthermore, the comparison between end-point deaminase reactions and the reference well (various 8-aza-adenosine concentrations but no TM0936 added) provided the calibration curve of fluorescence signal for the 8-aza-adenosine to 8-aza-ionisine

reaction. Using the *Ex/Em* pairs (282/360 and 292/360 nm), the data fit to the supplementary Eq. S10 provided the calibration parameters. These parameters are summarized in supplementary Table S2.

$$\Delta FLUO = a[\text{8-}aza\text{-}A]^2 + b[\text{8-}aza\text{-}A] + c \quad (\mathbf{S10})$$

Kinetic behavior for H4$_{(1-20)}$ against TbPRMT7 using 8-aza-SAM− The Excel file "*My 1-Step EZ-MTase Assay (FLUO) Acceptor Km.xlsx*" (*cf*. ESI) provides an exhaustive templates to help the users in data processing/analysis. Experiments were conducted following *Tb*PRMT7 protocol above. Briefly, the 250-μL reaction mixtures from a same row contained 25 mM phosphate buffer pH=7.60, 1 mM βME, 10% glycerol, 4 μM coupling deaminase TM0936, 805.2 nM *Tb*PRMT7 and various peptide concentrations (0−144.55 μM. The first well contained only 8-aza-SAM without any coupling enzyme, nor methyltransferase; in the second well, peptide acceptor was omitted to account for background signal −natural decomposition of 8-aza-SAM). Reactions started upon addition of cofactor (25.0 μM saturating final concentration) and absorbance was recorded. Initial rates were first corrected for background signal, then plotted against H4$_{(1-20)}$ concentrations. The data fit to the Michaelis-Menten equation S5 provided corresponding k_{cat} of 39 ± 2 h^{-1} and a K_m value of 71 ± 8 μM.

Detection of GNMT activity within liver extracts

Animals required for the study−Fischer 344 x Brown Norway (FBN) F1 hybrid male rats were obtained from the NIA aging rodent colony. All animals were individually housed and provided a standard chow diet (Purina 5001). Following a 4−6hr fast, animals were sacrificed under isoflurane anesthesia and the liver was rapidly freeze clamped, flash frozen in liquid nitrogen, and stored at -80 °C. All experiments were approved by the Institutional Animal Care and Use Committee (IACUC) at the Albert Einstein College of Medicine (IACUC Protocol #20150106).

Liver protein extraction−For total protein isolation, frozen liver samples were mechanically homogenized in an ice-cold non-denaturing lysis buffer (150 mM NaCl, 20 mM Tris-HCl (pH 7.4), 1% Triton X-100, 1 mM orthovanadate, 1 mM EDTA, 10 mM NaF, 1X protease inhibitor cocktail, and 1 mM PMSF), similar as previously described.[20] Tissue homogenates were subsequently cleared by centrifugation, and assayed for total protein content using the bicinchoninic acid (BCA) protein assay (Sigma, St. Louis, MO) with BSA as a standard.

Compatibility between lysis buffer and the 1-Step EZ-MTase assay−A master mix containing 1575 μL of 200 mM phosphate buffer pH 8.00, 525 μL of 80% glycerol, 210 μL of 100 mM βME, 56 μL of 200 mM GSH, 350 μL of 48.1 μM TM0936 and 534 μL of 591 μM SAM was prepared. A fixe 232-μL volume of master mix was combined with increasing concentration *Hs*GNMT (*e.g.* 0−100 nM) and water (to 285 μL final volume). Methyltransfer reactions started upon addition of glycine (15 μL, 400 mM) and 250 μL were transferred into a 96-well plate to further record UV absorbance at 263 nm (final reagents' concentrations: 75 mM phosphate, 10% glycerol, 5 mM βME, 2.5 mM GSH, 4 μM TM0936, 75 μM SAM and 20 mM glycine). Initial rates were first corrected for back-

ground signal, then plotted against *Hs*GNMT concentrations to yield linear calibration curve. A similar set of experiments was performed including a 10% volume of lysis buffer within the master mix. After correction for background, the initial rates were plotted against *Hs*GNMT concentrations to yield a new linear calibration curve. Both curves were superimposable, thus establishing the compatibility between lysis buffer and the 1-Step EZ-MTase assay.

Measurement of GNMT activity within biological samples: UV assay−A master mix containing 1125 μL of 200 mM phosphate buffer pH 8.00, 375 μL of 80% glycerol, 150 μL of 100 mM βME, 40 μL of 200 mM GSH, 250 μL of 48.1 μM TM0936 and 383 μL of 591 μM SAM was prepared. A fixe 232-μL volume of master mix was combined with increasing volumes of liver extract (*e.g.* 6, 12, 18 and 24 μL) and water (to 270 μL final volume). Likewise, a blank reaction containing 232 μL volume of master mix, 24 μL lysis buffer and water (to 270 μL final volume) was prepared. Methyltransfer reactions started upon addition of glycine (30 μL, 200 mM) and 250 μL were transferred into a 96-well plate to further record UV absorbance at 263 nm (final reagents' concentrations: 75 mM phosphate, 10% glycerol, 5 mM βME, 2.5 mM GSH, 4 μM TM0936, 75 μM SAM and 20 mM glycine). Initial rates were first corrected for background signal, then plotted against liver extract volumes to yield linear activity curve; the slope of this representation ($\mu M\ h^{-1}\ \mu L^{-1}$) was converted into GNMT activity and normalized to the amount of total protein originally present within liver extract (GNMT activity expressed in picomoles of sarcosine synthesized per minute and per milligram of total protein: $pmol\ min^{-1}\ mg^{-1}$).

Measurement of GNMT activity within biological samples: Radio assay−Quenching suspensions of charcoal were prepared according to a reported procedure with slight modification:[21] 1.00 g of acid-washed activated charcoal (Sigma-Aldrich, # C4386) was added to a 40-mL solution of glycine (10 mM) under continuous stirring (350 rpm). Aliquots of this suspension (200 μL) were transferred into 1.5 mL tubes. A 135-μL reaction mixture (Rx1) containing phosphate buffer (75 mM, pH 8.0), 10% glycerol, 5 mM βME, 2.5 mM GSH, 4 μM TM0936, 65 μM *cold* SAM and 10 μM *hot* SAM (~25 x 10^6 cpm of tritium; previously purified by HPLC) was prepared with 12.5-μL of liver extract. Likewise, two side reaction mixtures with and without 5 μM *Hs*GNMT (no liver extract added; Rx2 and Rx3, respectively) were prepared. Reactions started upon addition of glycine (15 μL of a 200 mM stock solution; 20 mM final concentration). At 5, 10, 20, 30, 40, 50, 60, 90 and 120 min, samples (15 μL) were taken from Rx1 and directly quenched into the tubes containing charcoal suspension. At 120 min, samples (15 μL) were taken from Rx2 and Rx3 and directly quenched into the tubes containing charcoal suspension. Quenched samples were spun down (10 min, 14.000 rpm, 20 °C) and a first round of clear supernatants (150 μL) was transferred into scintillation vials. A glycine solution (10 mM, 150 μL) was added to each quenching tubes to extract most of the radioactive sarcosine product. The suspensions were vortexed and spun down (10 min, 14.000 rpm, 20 °C); the second round of clear supernatants (150 μL) was transferred and combined with the first round into scintillation vials. After addition of scintillation liquid (10 mL; Ultima Gold, PerkinElmer), radioactivity was quantified using a Liquid Scintillation Analyzer (Tri-Carb 2810 TR; 0−26 keV channel). Sample from Rx2 and Rx3 provided the 100% completion and the radioactivity background signals, respectively. Further pro-

cessing of the original methyltransfer rate (cpm min^{-1}) provides GNMT activity expressed in picomoles of sarcosine synthesized per minute and per milligram of total protein (pmol min^{-1} mg^{-1}).

Supplementary Tables

	Name	Approach	Enzymes	Continuous	Detection Mode	Dynamic Range Lower	Dynamic Range Upper	pH Range	Salt Range	Sinefungin Compatible	Bio Samples	High Throughput Screening Multiwell Plate	High Throughput Screening Z′	Ref.
SAH-detection	*1-Step EZ-MTase*	SAH → SIH	TM0936 (SAH deaminase)	YES	UV (263 nm; SAM) FLUO (282/360 nm; 8-aza-SAM)	2.0 μM h^{-1} (4.0 μM TM0936)	1.0 x 10^4	5.0–10.0	Up to 2M NaCl	YES	YES	96-well tested 60–250 μL	> 0.75	This work
	Deamination Adenine	SAH → Adenine → Hx	MTAN, ADA	YES	UV (265 nm; SAM)	300 μM h^{-1}	ND	Tested at pH=8.0	ND	NO catabolized by MTAN	NO	1-cm quartz cuvette 3 mL	ND	30
		SAH → Adenine → NH_3 → NADP	MTAN, ADA, GLDH		UV (340 nm; SAM)	360 μM h^{-1}	ND	Tested at pH=7.5	YES			96-well tested 250 μL	ND	31
	FLUC-based Assays	SAH → Adenine → AMP → ATP	MTAN, APRT, PPDK, FLUC		LUM (570 nm; SAM)	60.0	ND	7.2–8.0	50% signal loss at 100 mM NaCl	NO catabolized by MTAN	NO	96-well tested	ND	28–29
		SAH → Adenosine → AMP → ATP	SAHH, AK, PPDK, FLUC							No inhibits SAHH	Adenine and phosphorylated Adenosines	50–100 μL	0.92	37
		Kinase Glo®	SAHH, AK, FLUC	NO		30.0 nM h^{-1}	ND	8.0–9.0				384-well tested 10 μL	0.60	36
	Homocysteine Detection	SAH → SRH → Hcy-SH → TNB	MTAN, LuxS	NO	UV (412 nm; SAM)	4.0 μM	ND	Tested at pH=7.5	ND	NO catabolized by MTAN	NO	96-well tested 250 μL	ND	32
		SAH → SRH → Hcy-SH → Thio Glo®	SAHH, Adenosine Deaminase,		FLUO 384/513 nm; SAM 493/516 nm; SAM	7.2 μM h^{-1}	ND			NO inhibits SAHH	Free thiol (GSH, cysteine)	96-well tested 50 μL	ND	33–34
	Specific Antibobies	SAH	NONE	NO	FLUO 480/535 nm; SAM	5.0 nM (Max SAM 3 μM)	25.0	Tested at pH=7.5	ND	ND	ND (unlikely)	384-well tested 50 μL	ND	38
		SAH → AMP	SAHH, AK		FLUO 635/670 nm; SAM	70–100 nM (SAM 0.2–50 μM)	ND			Tested		384/1536-well tested < 20 μL	0.60	35
Methyl Mark	*Radioactive Assays*	^{3}H-*methyl* or ^{14}C-*methyl* SAM substrate	NONE	NO	^{3}H-*methyl* or ^{14}C-*methyl* product various filter assays	250 (10) cpm h^{-1} (nmol h^{-1})	ND	various	YES	YES	YES	various	ND	22–25
	Specific Antibobies	Recognize methyl mark			AlphaLISA (680/615 nm)	10 nM (H3K4me1/me2)	500	pH=8.8	ND	YES	ND (unlikely)	384-well tested < 25 μL	> 0.70	26
					FRET (490/520 nm)	various		pH=8.0		ND			ND	27

Table S1 A summary of the 1-Step EZ-MTase performances and a comparison with other assays capable of detecting methyltransferase activities. Coupling enzymes: MTAN (5′-methylthioadenosine/*S*-adenosylhomocysteine nucleosidase), ADA (adenine deaminase), GLDH (glutamate dehydrogenase), APRT (adenine phosphoribosyltransferase), PPDK (pyruvate phosphate dikinase), FLUC (firefly luciferase), SAHH (*S*-adenosylhomocysteine hydrolase), AK (adenosine kinase) LuxS (*S*-ribosylhomocysteine lyase). Detection modes: UV (UV−visible absorbance), FLUO (fluorescence), LUM (luminescence). ND: not determined.

	ΔFLUO (RFU) =	a [8-aza-A]^2	+b [8-aza-A]	+c
CURVES	*Ex/Em* 282/360 nm			
	pH=5.00	-3.4 ± 0.2	450 ± 4	185
	pH=9.50	-3.2 ± 0.1	414 ± 2	185
	Ex/Em 282/360 nm			
	pH=5.00	-1.3 ± 0.1	253 ± 3	118
	pH=9.50	-1.32 ± 0.06	236 ± 1	118

Table S2 Parameters for data fit regarding calibration of fluorescence signal for the 8-aza-adenosine to 8-aza-inosine reaction. Experiments performed at pH=5.00 and pH=9.50.

Supplementary Figures

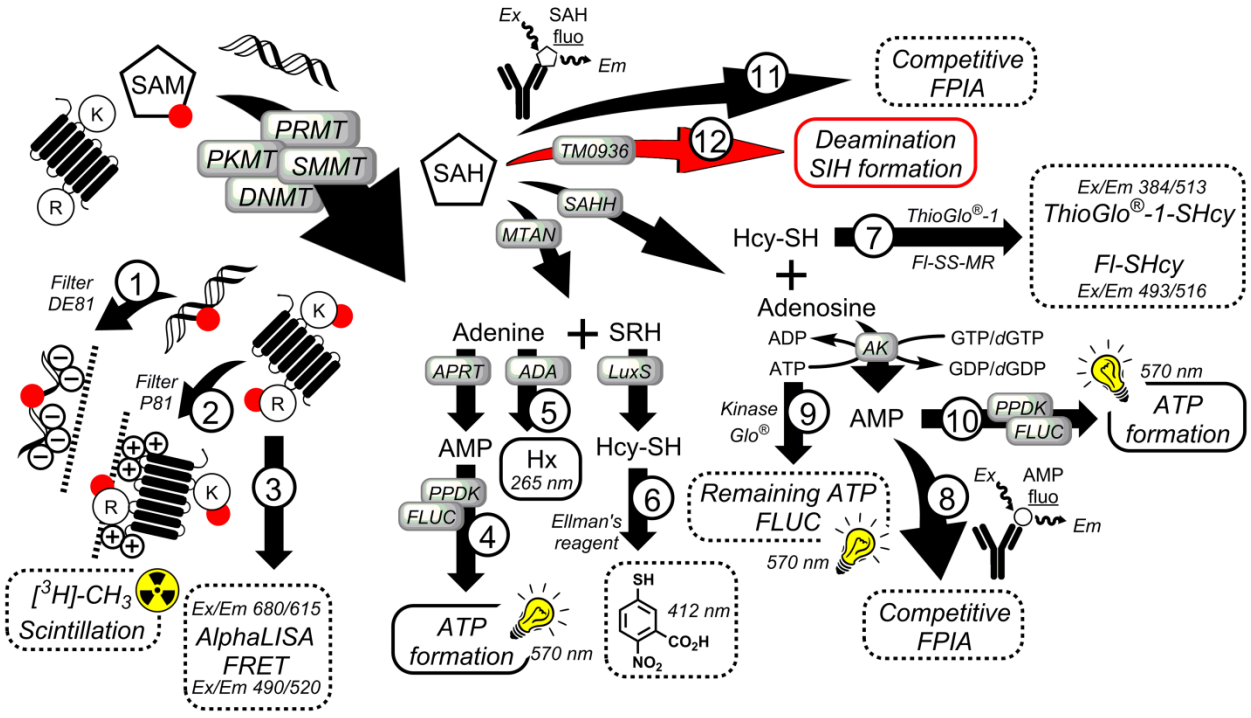

Fig. S1 The detection of methyltransfer reactions: a summary of assays currently available. The protein lysine-, arginine-, DNA and small molecule methyltransferases (PKMT, PRMT, DNMT and SMMT, respectively) deposit the methyl mark (red sphere) onto specific acceptors using the universal methyl donor *S*-adenosyl-L-methionine (SAM). These reactions lead to the by-product *S*-adenosyl-L-homocysteine (SAH). *In vitro*, analysis of methyltransfer is achieved via two major strategies. The first approach involves methyl mark detection (methods **1**−**3**). Then, SAH detection may be performed through both continuous and discontinuous assays (bold and dotted frames, respectively; methods **4**−**12**).

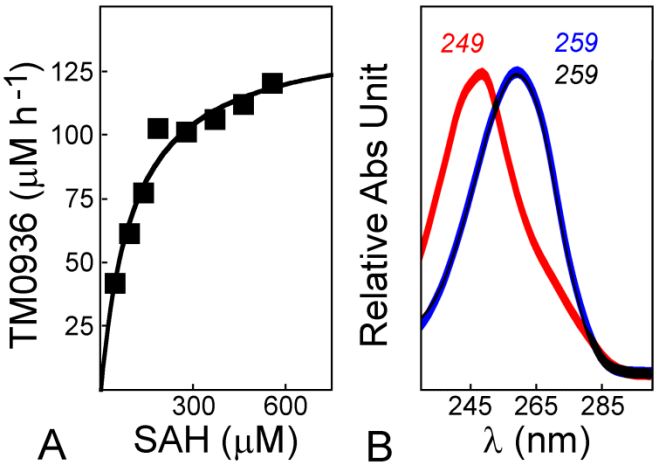

Fig. S2 Kinetic properties of the deaminase TM0936. (**A**) Determination of the K_m and k_{cat} for the SAH substrate through loss of absorbance at 263 nm. Deaminase reactions (60 μL) started upon addition of TM0936 (17.5 nM) in presence of SAH (46−556 μM) at pH=8.00 (25 mM phosphate, 10% glycerol, 1 mM βME). Initial rates were fitted to Eq. S5. (**B**) Spectral signatures for the *S*-adenosyl-L-methionine cofactor (SAM; blue), *S*-adenosyl-L-homocysteine (SAH; black) and *S*-adenosyl-L-inosine (SIH; red). While SAM and SAH spectra are superimposable with maximum absorption wavelength at 259 nm, a blueshift is observed upon the SAH-deamination leading to SIH (maximum absorption wavelength at 249 nm; pH=6.00).

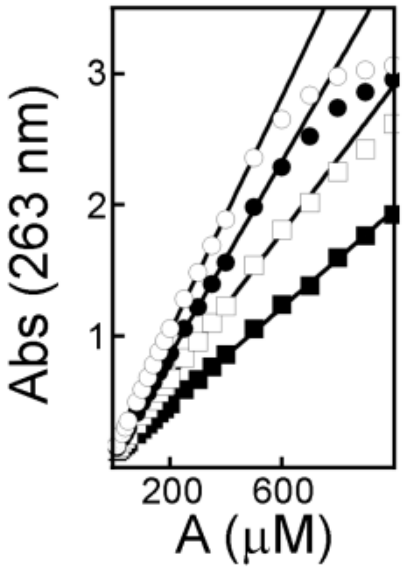

Fig. S3 The linear relationship between absorbance and concentration with 1-Step EZ-MTase assay. The absorbance from different adenosine standard solutions (A; 0−1000 μM) was recorded at 263 nm with a Spectramax M5 plate reader in UV-Star 96-well flat bottom plate (Greiner Bio-One, #655801). Wells were filled with either 50-, 75-, 100- or 125-μL standard solutions (black squares, white squares, black circles and white circles, respectively). All solutions contained 10% glycerol and 1 mM βME. Absorbance/concentration relationship remains linear for absorbance below 2.

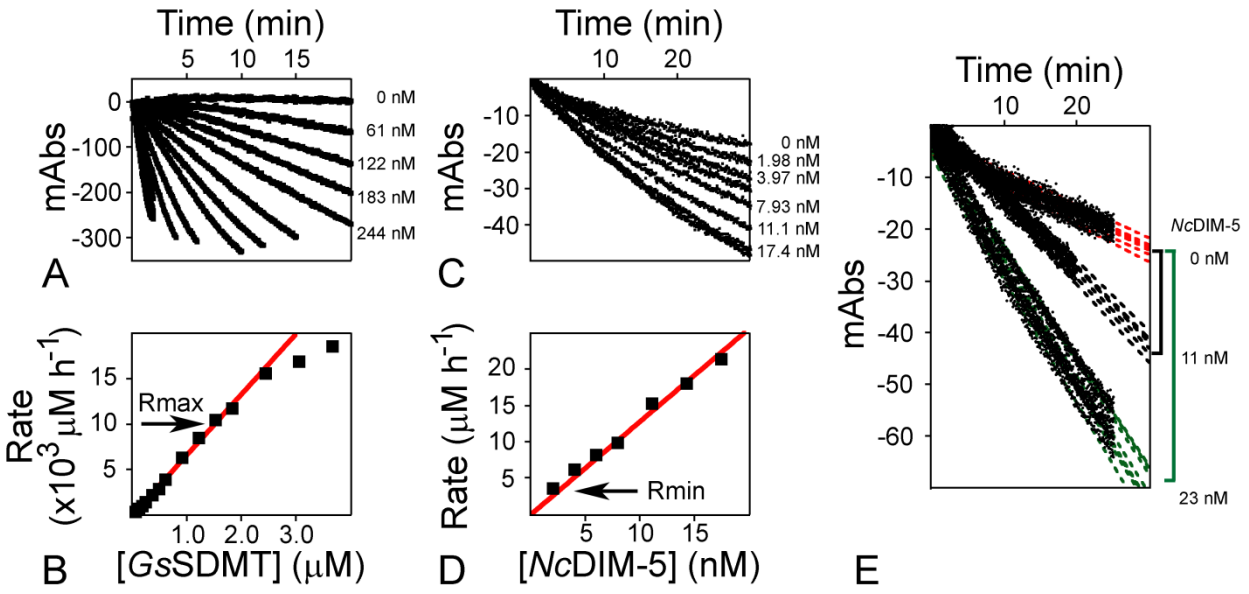

Fig. S4 The dynamic range of SAH-detection with the 1-Step EZ-MTase assay. (**A**) Experimental set-up to determine the upper limit of SAH-detection. Increasing concentrations of *Gs*SDMT (0−3.66 μM) were used to methylate sarcosine. The loss of absorbance at 263 nm reports on methyltransfer. (**B**) Upper limit of SAH-detection. Initial rates for sarcosine methylation were plotted against *Gs*SDMT concentrations. The relationship between these two parameters is linear (red trace) below the upper limit of SAH-detection (Rmax; black arrow). Above Rmax, the deamination catalyzed by TM0936 is rate limiting and the loss of absorbance at 263 nm does not accurately report on the methyltransfer. (**C**) Experimental set-up to determine the lower limit of SAH-detection. Decreasing concentrations of *Nc*DIM-5 (17.45−0 nM) were used to methylate $H3_{(1-53)}$ peptide. Methyltransfer rates were recorded following loss of absorbance at 263 nm. (**D**) Lower limit of SAH-detection. Initial rates for $H3_{(1-53)}$ methylation were plotted against *Nc*DIM-5 concentrations. Although the relationship between these two parameters is linear across the whole range of methyltransferase concentrations (red trace), a lower limit of SAH-detection (Rmin; black arrow) is established above the background signal. Below Rmin, the discrimination between methyltransfer and natural decomposition of SAM is inaccurate. (**C**) Determination of the *Z′*-factor. Eight replicates of methylation reactions were recorded at various methyltransferase concentrations. Replicates display variability in reaction rates (dotted fitted lines). Furthermore, higher separation bands (black and green brackets) with the background signal (red dotted fitted lines) are achieved at higher methyltransferase concentrations.

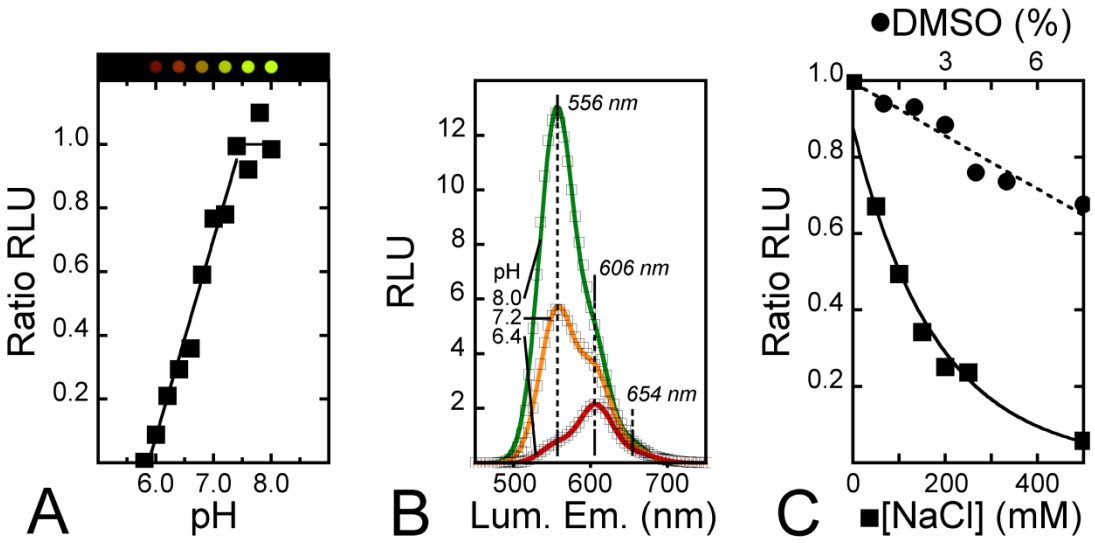

Fig. S5 The drawbacks of luciferase-based coupled assays. (**A**) The light-output produced by recombinant *Photinus pyralis* luciferase (FLUC) is optimum within a narrow pH-range (7.40−8.00; bright green light). At lower pH values, the luminescence drastically decreases as it shifts towards a red emission spectrum. (**B**) Spectral analysis of the FLUC luminescence. The light generated upon luciferin oxidation is a combination of three spectral components with maximum emission at 556, 606 and 654 nm. Luminescence (RLU) was recorded and analyzed for pH 8.00, 7.20 and 6.40 (green, orange and red curve, respectively). Lowering solutions pH mostly affects the green component of the luminescence spectrum, thus reducing the sensitivity of luciferase-based coupled assays. (**C**) FLUC luminescence is impaired by the additives DMSO and NaCl. Half the luminescence produced by FLUC was lost upon addition of sodium chloride (100 mM; black squares). Likewise, DMSO –often used to dissolve molecules from screening libraries– reduces light-output produced by this enzyme (black circles).

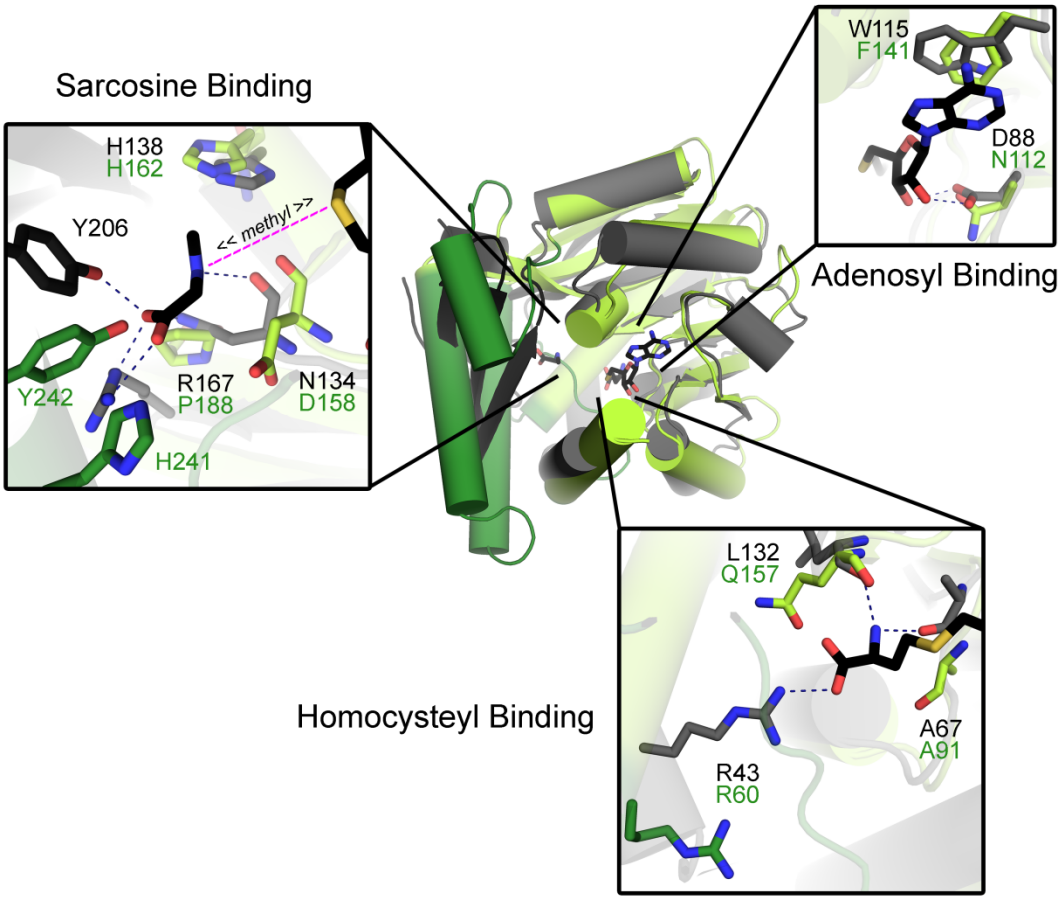

Fig. S6 Ribbon diagram superimposition of the *Gs*SDMT and *Mp*GSMT structures. The apo-form of sarcosine dimethylglycine *N*-methyltransferase from *Galdieria sulphuraria* (*Gs*SDMT, green representation; PDB: **2O57**) was aligned with the SAH•sarcosine complex of glycine sarcosine *N*-methyltransferase from *Methanohalophilus portucalensis* (*M*pGSMT, grey representation; PDB: **5HIL**). Both structures display a good alignment of their *N*-terminus (light shades) where the SAM binding site is localized. The first insert labelled “adenosyl binding” highlights key residues involved in the recognition of cofactor nucleoside moiety: these include π-stacking with W115 and stabilization at the ribosyl level through hydrogen bond with D88; the residues F141 and N112 from *Gs*SDMT are predicted to be homologous. Furthermore, the insert labelled “homocysteyl binding” depicts additional residues involved in stabilization of the cofactor. The amino-acids R60, A91 and Q157 from *Gs*SDMT appear to be homologous to R43, A67 and L132 from *Mp*GSMT, thus predicted to interact with the homocysteyl moiety from SAM/SAH. The last insert “sarcosine binding” highlights the residues essential for acceptor recognition and relevant to the methyltransfer catalysis (pink dotted line). This binding site is located within the most divergent region of the structures (dark shades): the *C*-terminus. Like its Y206 homolog in *Mp*GSMT, residue Y242 from *Gs*SDMT is likely stabilizing sarcosine via hydrogen bond with the carboxylate tail. The histidine H162 in *Gs*SDMT, also present in *Mp*GSMT (H138) may influence methyltransfer rate.

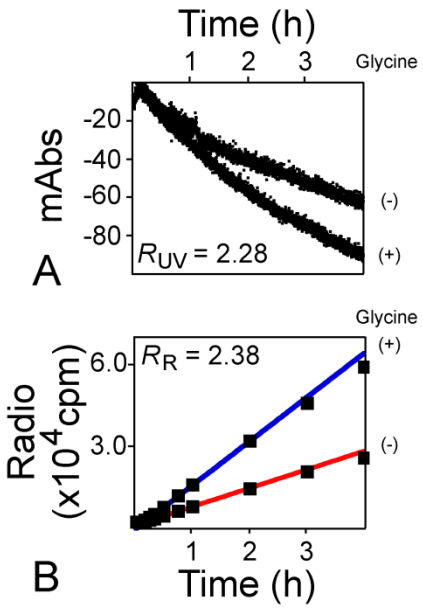

Fig. S7 Liver extracts require saturating levels of glycine to provide optimum signal output during GNMT activity measurement. (**A**) Detection of GNMT activity with 1-Step EZ-MTase assay. Two 300 μL reactions containing liver extract (24 μL), SAM (75 μM), βME (5 mM), GSH (2.5 mM), 10% glycerol and TM0936 (4 μM) were carried out at pH=8.00 (75 mM phosphate), with and without glycine (20 mM; + and – signs, respectively). Decrease of absorbance was recorded over four hours at 263 nm in a 96-well plate using 250 μL volumes. (**B**) Detection of GNMT activity with radioactive assay. Two 150 μL reactions containing liver extract (12 μL), SAM (75 μM; 14 x 10^6 cpm tritium), βME (5 mM), GSH (2.5 mM), 10% glycerol and TM0936 (4 μM) were carried at pH=8.00 (75 mM phosphate), with and without glycine (20 mM; + and – signs, respectively). Aliquots (15 μL) were quenched upon charcoal treatment at 10, 15, 20, 30, 45, 60, 120, 180 and 240 min; radioactive sarcosine product, was quantified by scintillation counting (cpm). Supported by both the 1-Step EZ-MTase and the radioactive assay, the endogenous glycine from liver extract is sufficient to detect GNMT activity; a 20 mM substrate concentration is required to saturate the methyltransferase. Upon glycine saturation, a 2.28- and 2.38-fold increase in GNMT activity is detected by the 1-Step EZ-MTase and the radioactive assay, respectively.

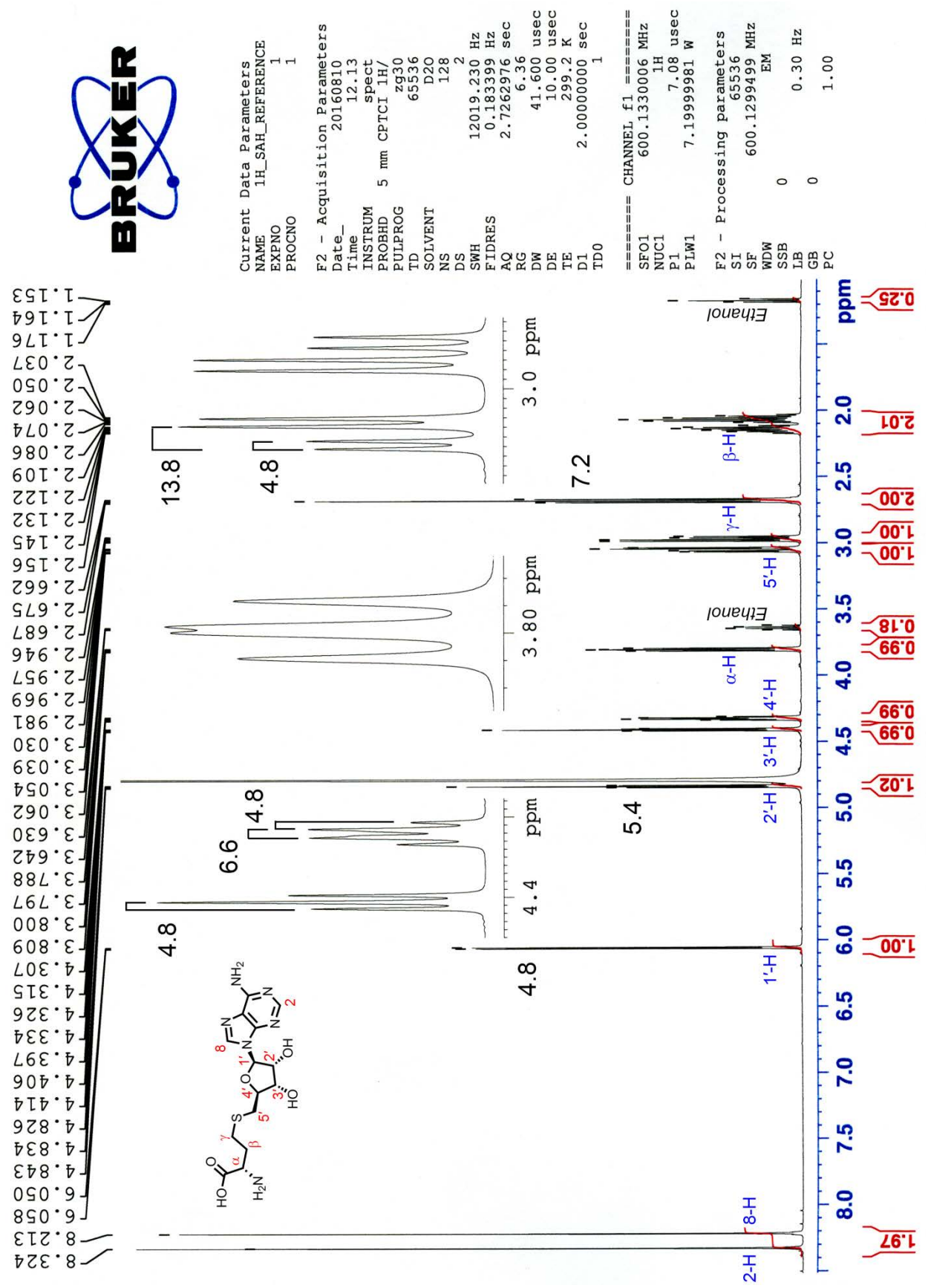
Current Data Parameters
NAME 1H_SAH_REFERENCE
EXPNO 1
PROCNO 1
F2 - Acquisition Parameters
Date_ 20160810
Time 12.13
INSTRUM spect
PROBHD 5 mm CPTCI 1H/
PULPROG zg30
TD 65536
SOLVENT D2O
NS 128
DS 2
SWH 12019.230 Hz
FIDRES 0.183399 Hz
AQ 2.7262976 sec
RG 6.36
DW 41.600 usec
DE 10.00 usec
TE 299.2 K
D1 2.00000000 sec
TD0 1
======== CHANNEL f1 ========
SFO1 600.1330006 MHz
NUC1 1H
P1 7.08 usec
PLW1 7.19999981 W
F2 - Processing parameters
SI 65536
SF 600.1299499 MHz
WDW EM
SSB 0
LB 0.30 Hz
GB 0
PC 1.00
13.8
4.8
3.0 ppm
7.2
4.8
3.80 ppm
Ethanol
4.8
6.6
4.8
4.4 ppm
5.4
4.8
Ethanol
2-H
8-H
1'-H
2'-H
3'-H
4'-H
α-H
5'-H
γ-H
β-H
1.97
1.00
1.02
0.99
0.99
0.18
0.99
1.00
1.00
2.00
2.01
0.25
ppm

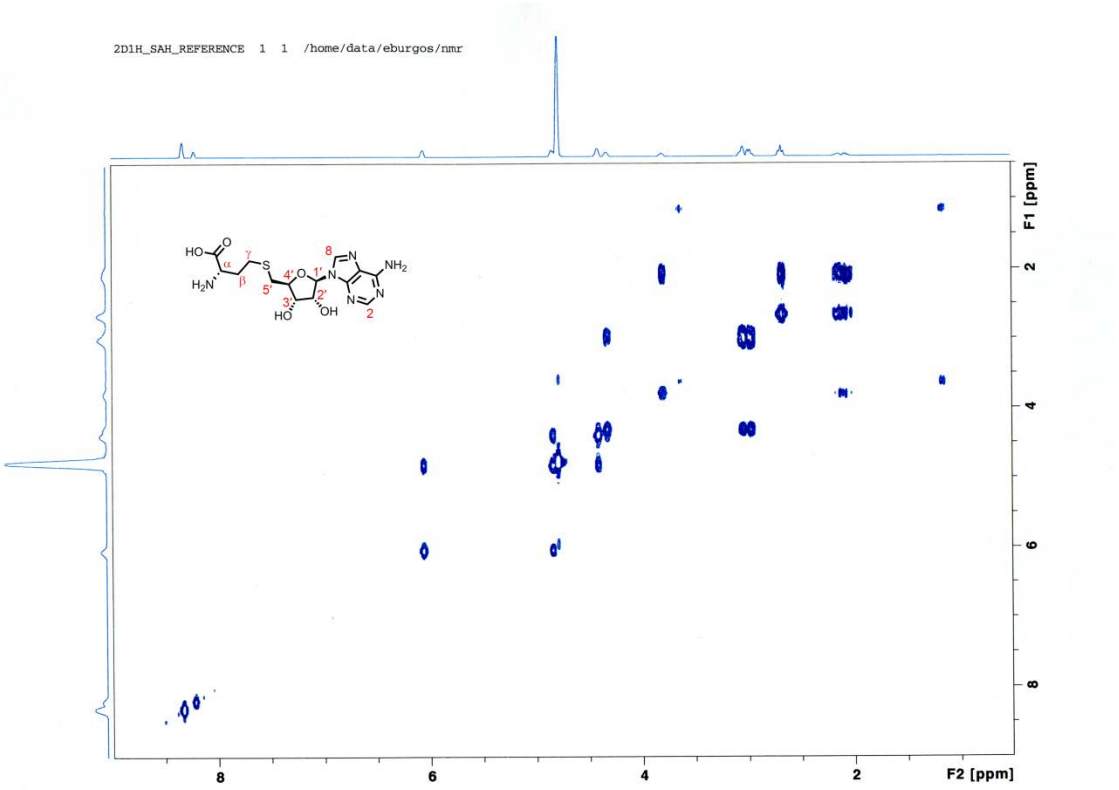
2D1H_SAH_REFERENCE 1 1 /home/data/eburgos/nmr
F1 [ppm]
F2 [ppm]

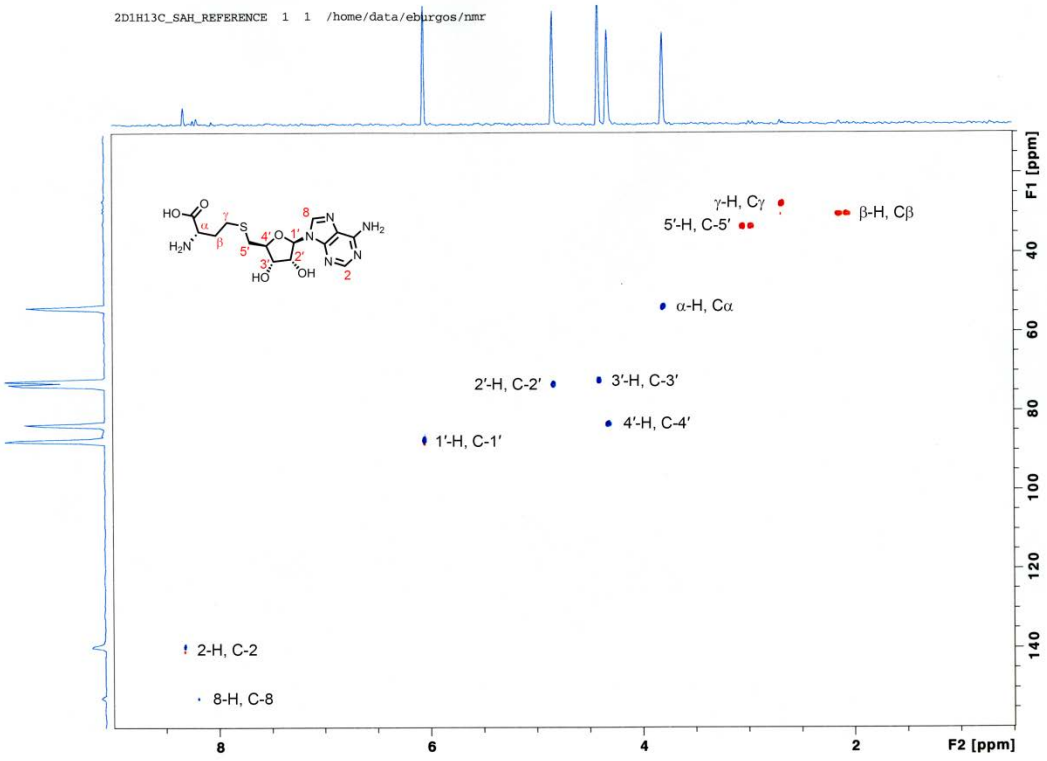
2D1H13C_SAH_REFERENCE 1 1 /home/data/eburgos/nmr
γ-H, Cγ
β-H, Cβ
5′-H, C-5′
α-H, Cα
2′-H, C-2′
3′-H, C-3′
4′-H, C-4′
1′-H, C-1′
2-H, C-2
8-H, C-8
F1 [ppm]
F2 [ppm]

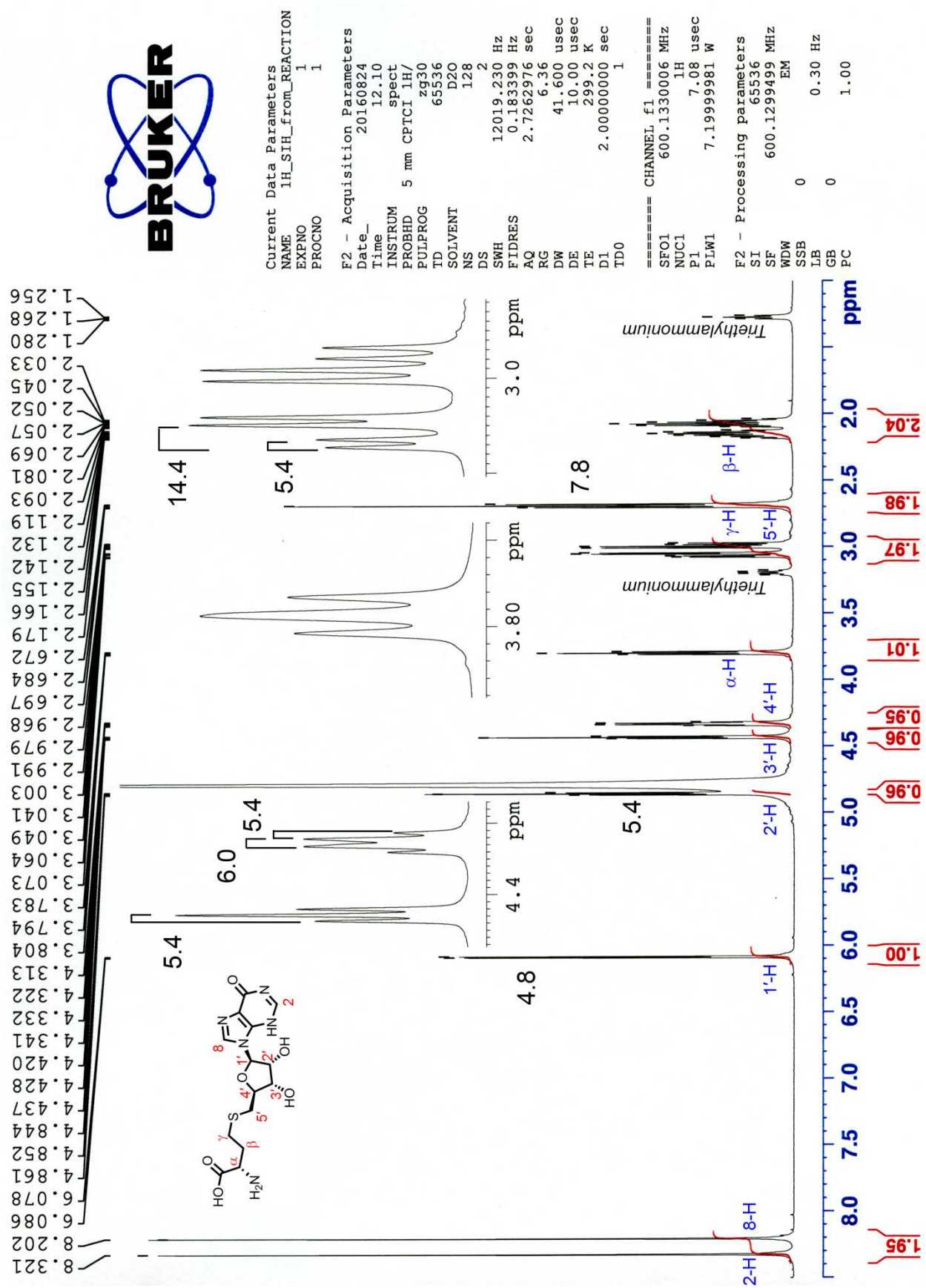
Current Data Parameters
NAME 1H_SIH_from_REACTION
EXPNO 1
PROCNO 1
F2 - Acquisition Parameters
Date_ 20160824
Time 12.10
INSTRUM spect
PROBHD 5 mm CPTCI 1H/
PULPROG zg30
TD 65536
SOLVENT D2O
NS 128
DS 2
SWH 12019.230 Hz
FIDRES 0.183399 Hz
AQ 2.7262976 sec
RG 6.36
DW 41.600 usec
DE 10.00 usec
TE 299.2 K
D1 2.00000000 sec
TD0 1
======== CHANNEL f1 ========
SFO1 600.1330006 MHz
NUC1 1H
P1 7.08 usec
PLW1 7.19999981 W
F2 - Processing parameters
SI 65536
SF 600.1299499 MHz
WDW EM
SSB 0
LB 0.30 Hz
GB 0
PC 1.00
Triethylammonium
Triethylammonium
2-H
8-H
1'-H
2'-H
3'-H
4'-H
α-H
5'-H
γ-H
β-H
ppm

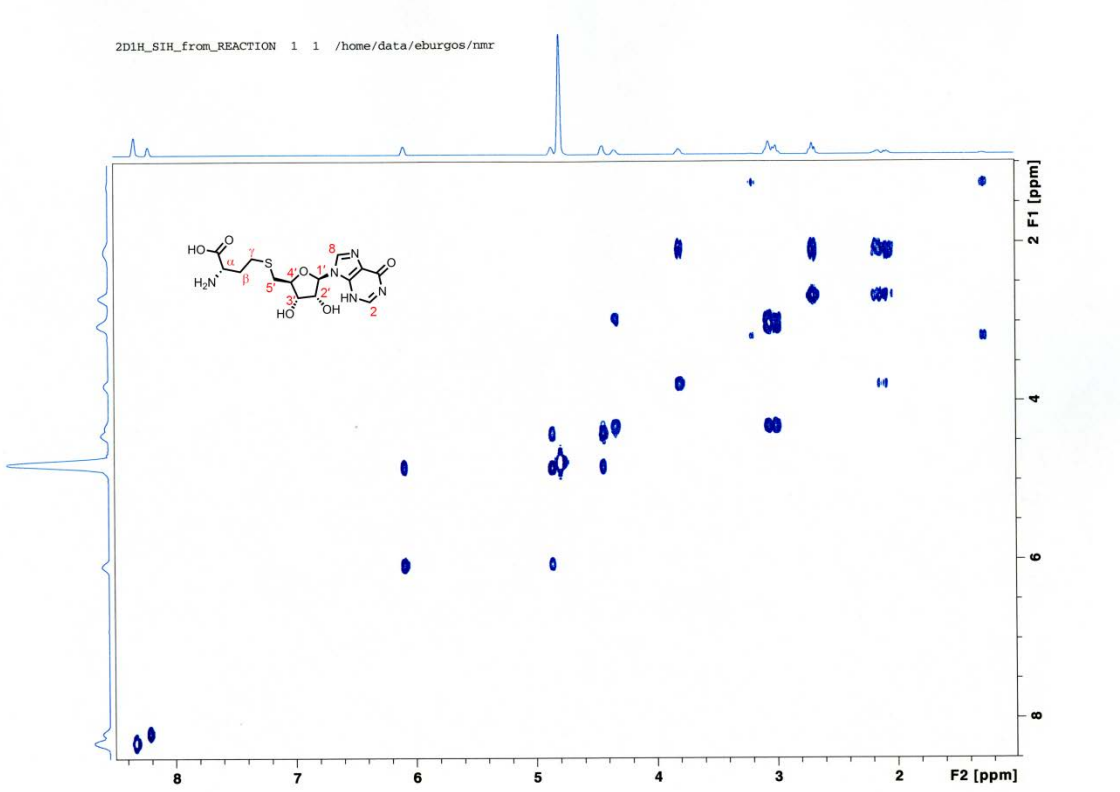
2D1H_SIH_from_REACTION 1 1 /home/data/eburgos/nmr
F2 [ppm]
F1 [ppm]

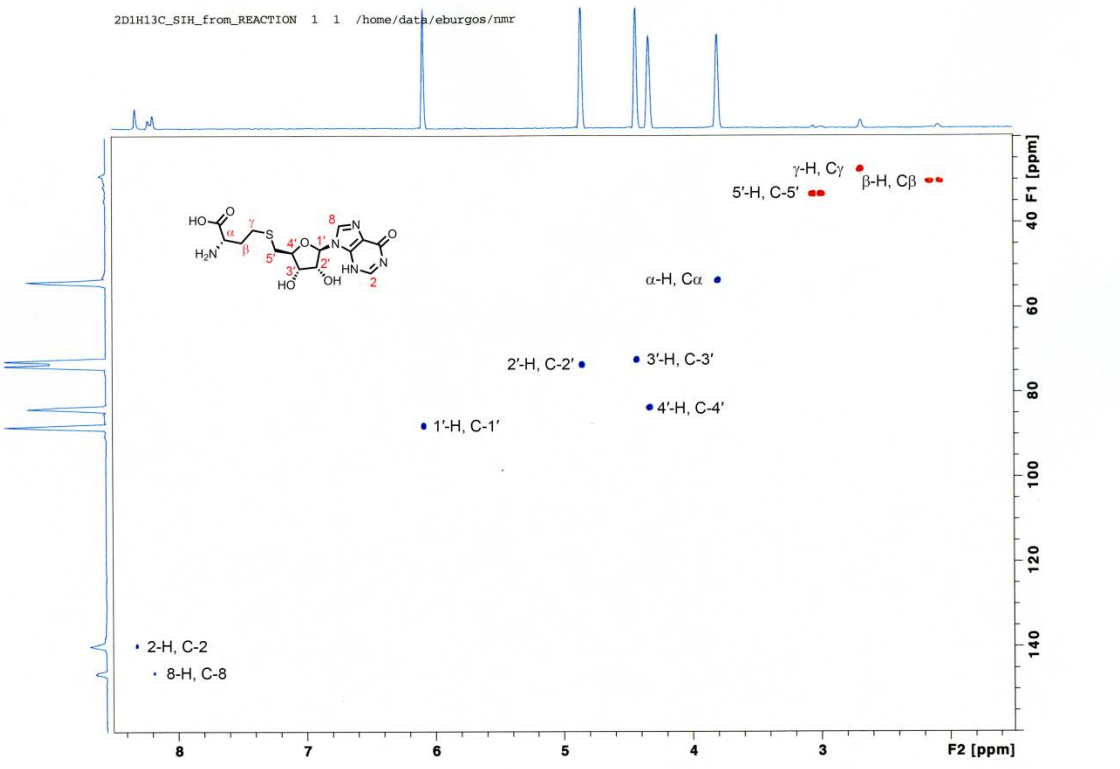
2D1H13C_SIH_from_REACTION 1 1 /home/data/eburgos/nmr
γ-H, Cγ
β-H, Cβ
5′-H, C-5′
α-H, Cα
2′-H, C-2′
3′-H, C-3′
4′-H, C-4′
1′-H, C-1′
2-H, C-2
8-H, C-8
F2 [ppm]
F1 [ppm]

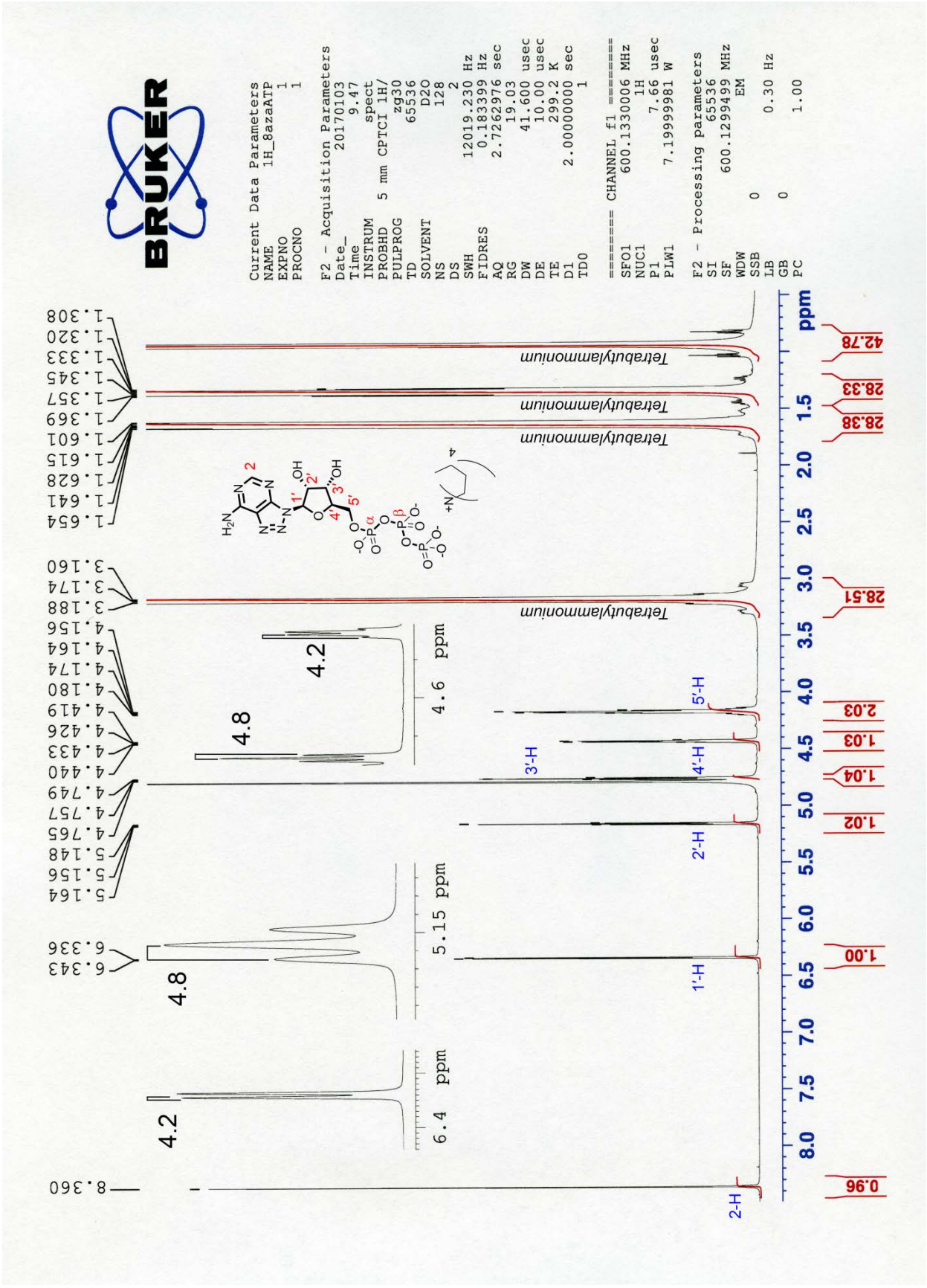
Current Data Parameters
NAME 1H_8azaATP
EXPNO 1
PROCNO 1
F2 - Acquisition Parameters
Date_ 20170103
Time 9.47
INSTRUM spect
PROBHD 5 mm CPTCI 1H/
PULPROG zg30
TD 65536
SOLVENT D2O
NS 128
DS 2
SWH 12019.230 Hz
FIDRES 0.183399 Hz
AQ 2.7262976 sec
RG 19.03
DW 41.600 usec
DE 10.00 usec
TE 299.2 K
D1 2.00000000 sec
TD0 1
======== CHANNEL f1 ========
SFO1 600.1330006 MHz
NUC1 1H
P1 7.66 usec
PLW1 7.19999981 W
F2 - Processing parameters
SI 65536
SF 600.1299499 MHz
WDW EM
SSB 0
LB 0.30 Hz
GB 0
PC 1.00
Tetrabutylammonium
Tetrabutylammonium
Tetrabutylammonium
Tetrabutylammonium
2-H
1'-H
2'-H
3'-H
4'-H
5'-H
ppm
42.78
28.33
28.38
28.51
2.03
1.03
1.04
1.02
1.00
0.96

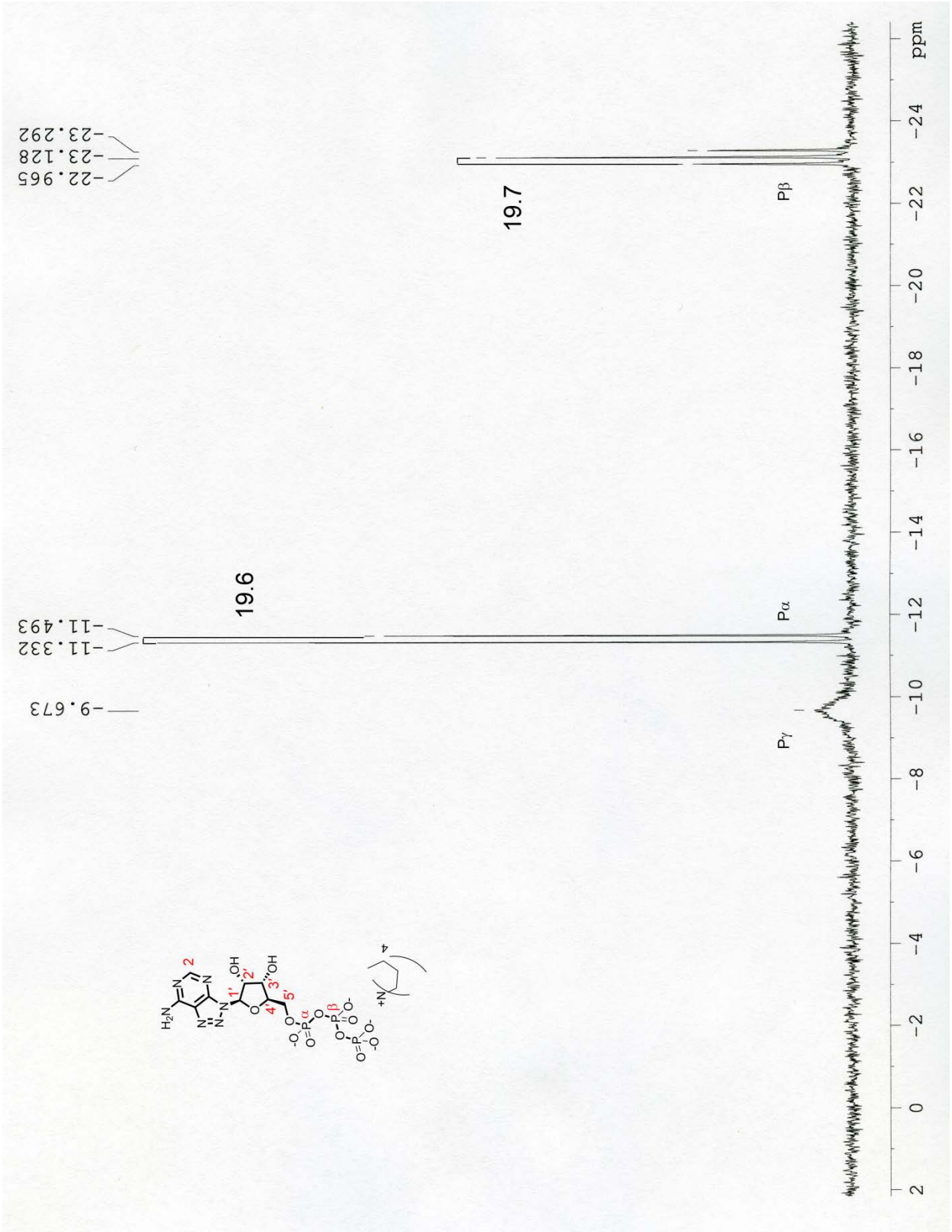
-22.965
-23.128
-23.292
19.7
Pβ
19.6
-11.332
-11.493
Pα
-9.673
Pγ
ppm
2
0
-2
-4
-6
-8
-10
-12
-14
-16
-18
-20
-22
-24

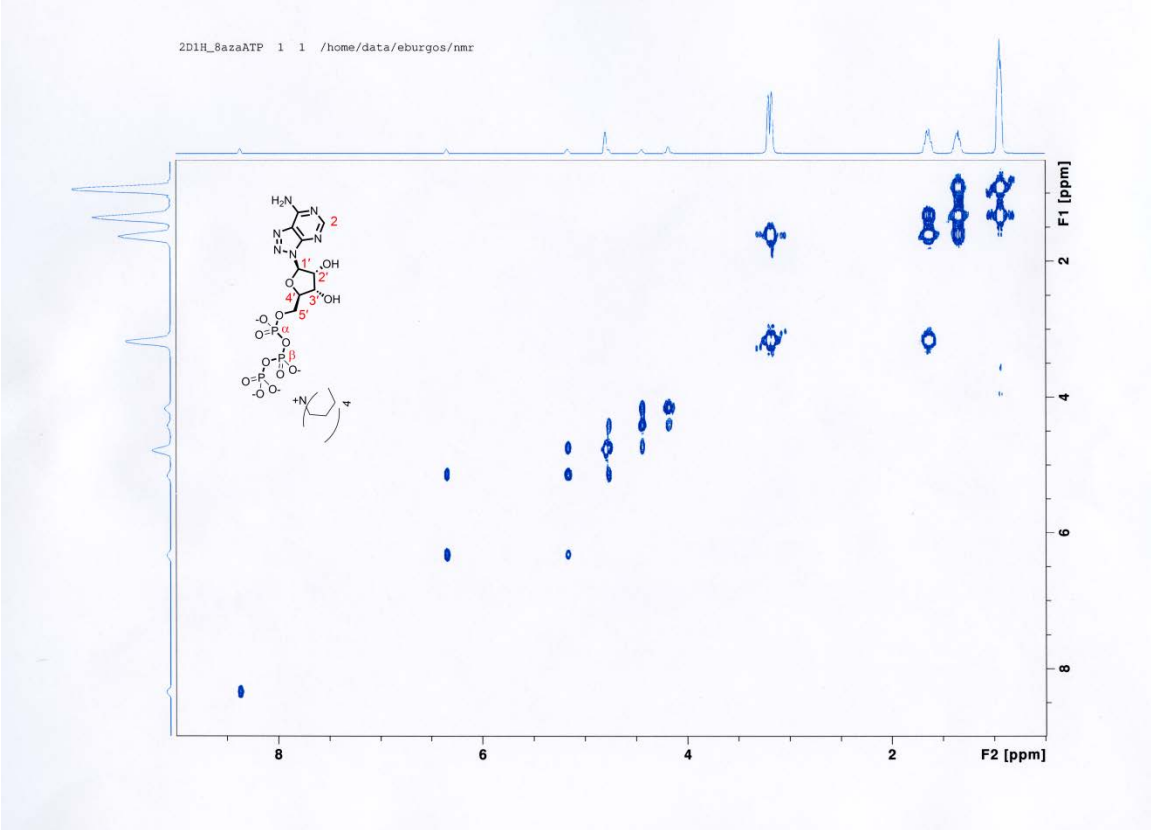
2D1H_8azaATP 1 1 /home/data/eburgos/nmr
F1 [ppm]
F2 [ppm]
8
6
4
2

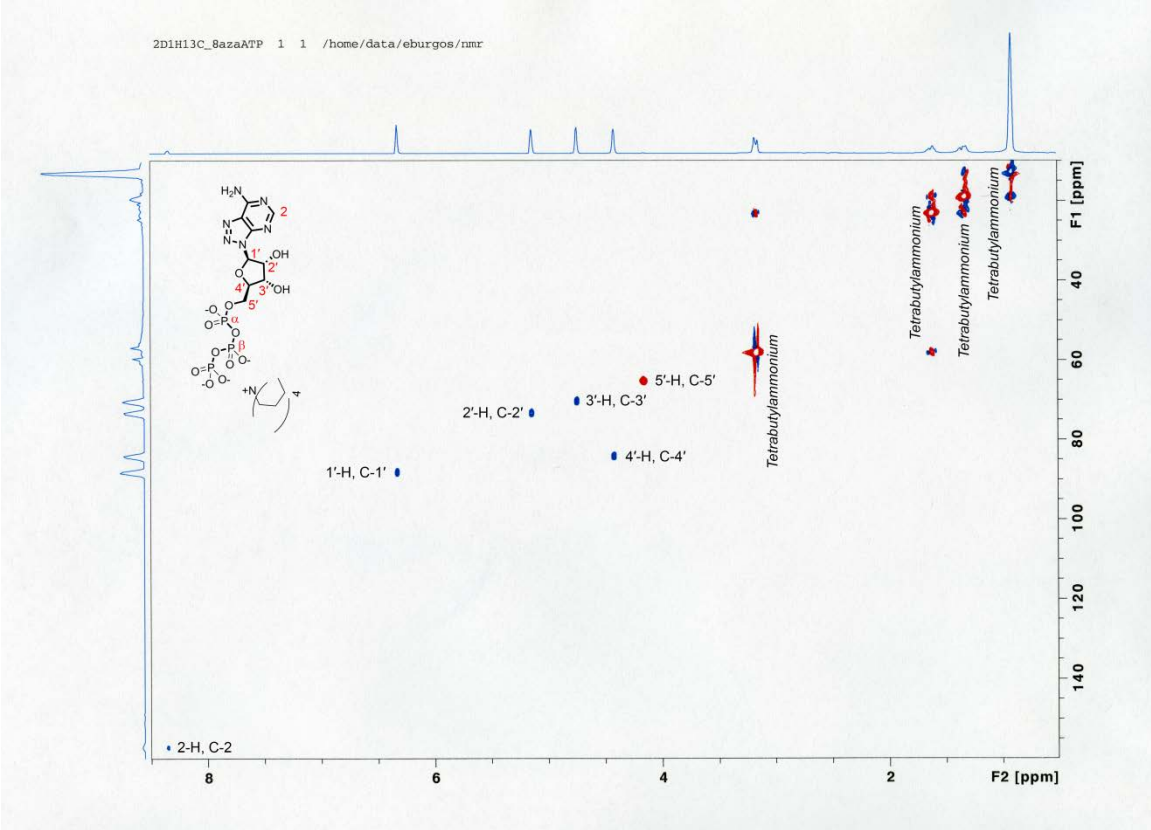
2D1H13C_8azaATP 1 1 /home/data/eburgos/nmr
F1 [ppm]
F2 [ppm]
Tetrabutylammonium
Tetrabutylammonium
Tetrabutylammonium
Tetrabutylammonium
5′-H, C-5′
3′-H, C-3′
2′-H, C-2′
4′-H, C-4′
1′-H, C-1′
2-H, C-2

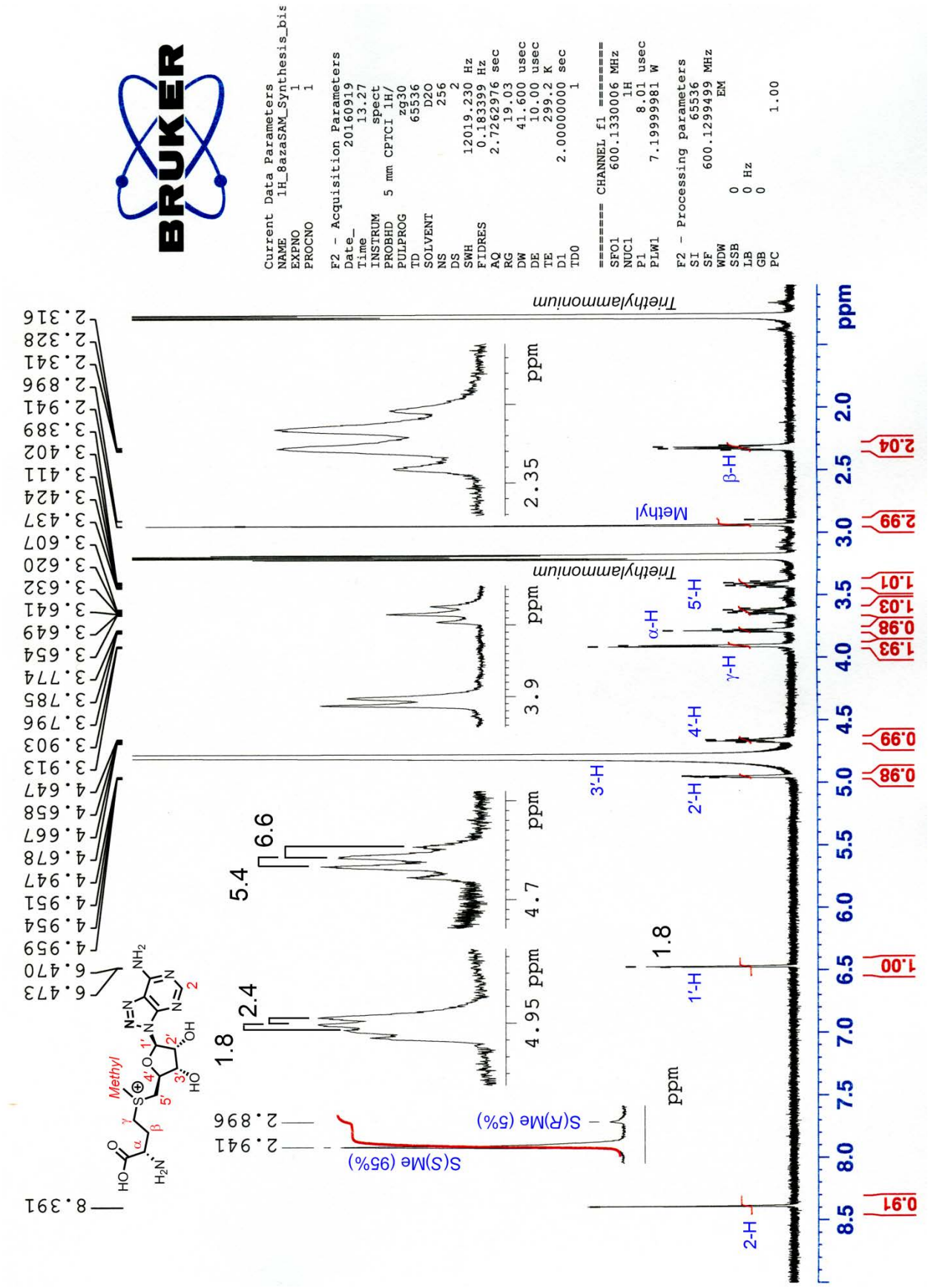
Current Data Parameters
NAME 1H_8azaSAM_Synthesis_bis
EXPNO 1
PROCNO 1
F2 - Acquisition Parameters
Date_ 20160919
Time 13.27
INSTRUM spect
PROBHD 5 mm CPTCI 1H/
PULPROG zg30
TD 65536
SOLVENT D2O
NS 256
DS 2
SWH 12019.230 Hz
FIDRES 0.183399 Hz
AQ 2.72629760 sec
RG 19.03
DW 41.600 usec
DE 10.00 usec
TE 299.2 K
D1 2.00000000 sec
TD0 1
======== CHANNEL f1 ========
SFO1 600.1330006 MHz
NUC1 1H
P1 8.01 usec
PLW1 7.19999981 W
F2 - Processing parameters
SI 65536
SF 600.1299499 MHz
WDW EM
SSB 0
LB 0 Hz
GB 0
PC 1.00
Triethylammonium
Methyl
β-H
2.35
ppm
Triethylammonium
α-H
5'-H
γ-H
4'-H
3.9
ppm
3'-H
2'-H
1'-H
1.8
4.95 ppm
4.7
ppm
5.4
6.6
2.4
1.8
ppm
S(S)Me (95%)
S(R)Me (5%)
2.941
2.896
8.391
2-H
Methyl
ppm
2.04
2.99
1.01
1.03
0.98
1.93
0.99
0.98
1.00
0.91

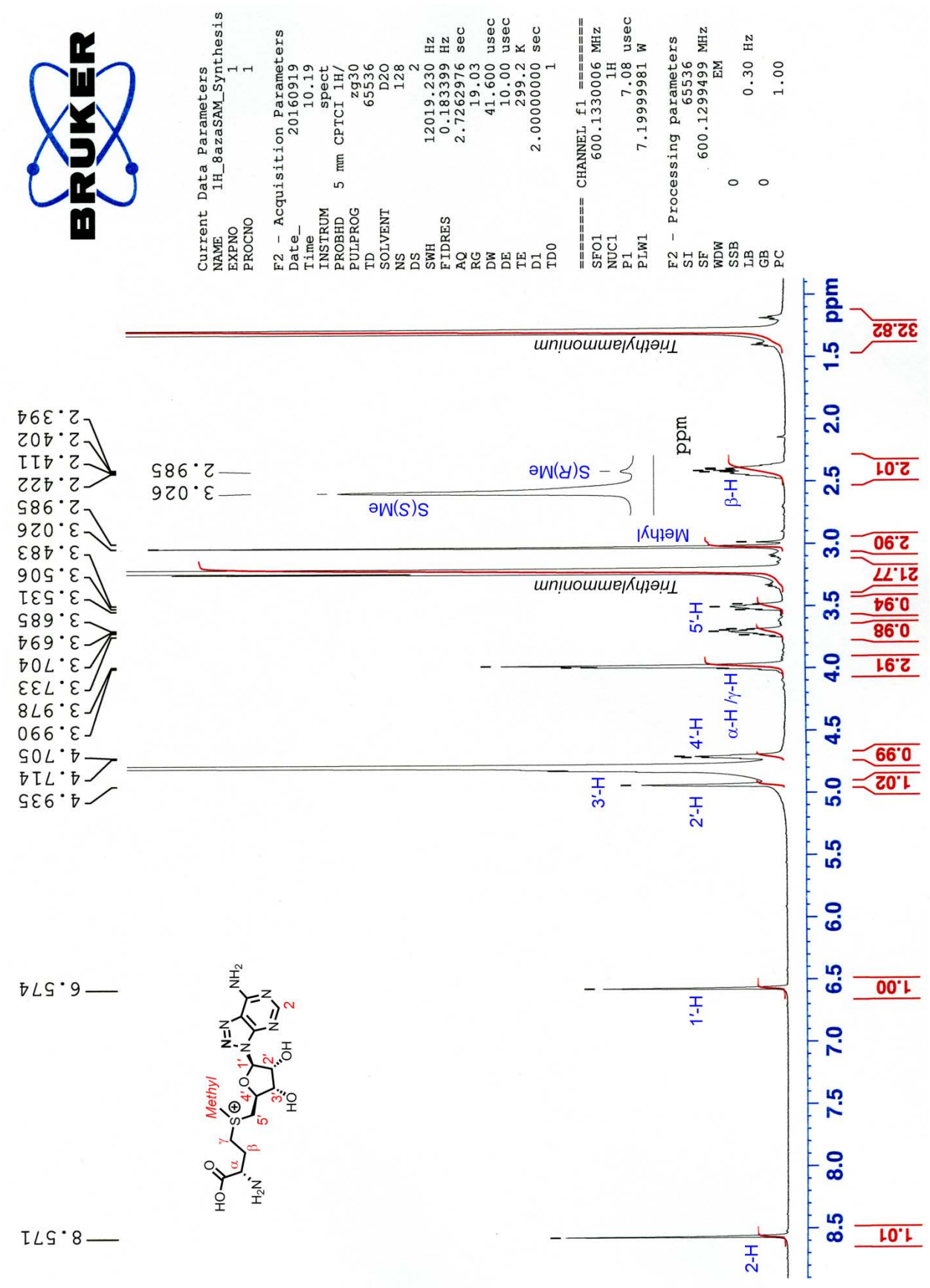
Current Data Parameters
NAME 1H_8azaSAM_Synthesis
EXPNO 1
PROCNO 1
F2 - Acquisition Parameters
Date_ 20160919
Time 10.19
INSTRUM spect
PROBHD 5 mm CPTCI 1H/
PULPROG zg30
TD 65536
SOLVENT D2O
NS 128
DS 2
SWH 12019.230 Hz
FIDRES 0.183399 Hz
AQ 2.7262976 sec
RG 19.03
DW 41.600 usec
DE 10.00 usec
TE 299.2 K
D1 2.00000000 sec
TD0 1
======== CHANNEL f1 ========
SFO1 600.1330006 MHz
NUC1 1H
P1 7.08 usec
PLW1 7.19999981 W
F2 - Processing parameters
SI 65536
SF 600.1299499 MHz
WDW EM
SSB 0
LB 0.30 Hz
GB 0
PC 1.00
Triethylammonium
Methyl
S(S)Me
S(R)Me
β-H
5'-H
α-H /γ-H
4'-H
3'-H
2'-H
1'-H
2-H
Methyl
ppm
32.82
2.01
2.90
21.77
0.94
0.98
2.91
0.99
1.02
1.00
1.01
8.571
6.574
4.935
4.714
4.705
3.990
3.978
3.733
3.704
3.694
3.685
3.531
3.506
3.483
3.026
2.985
2.422
2.411
2.402
2.394
3.026
2.985

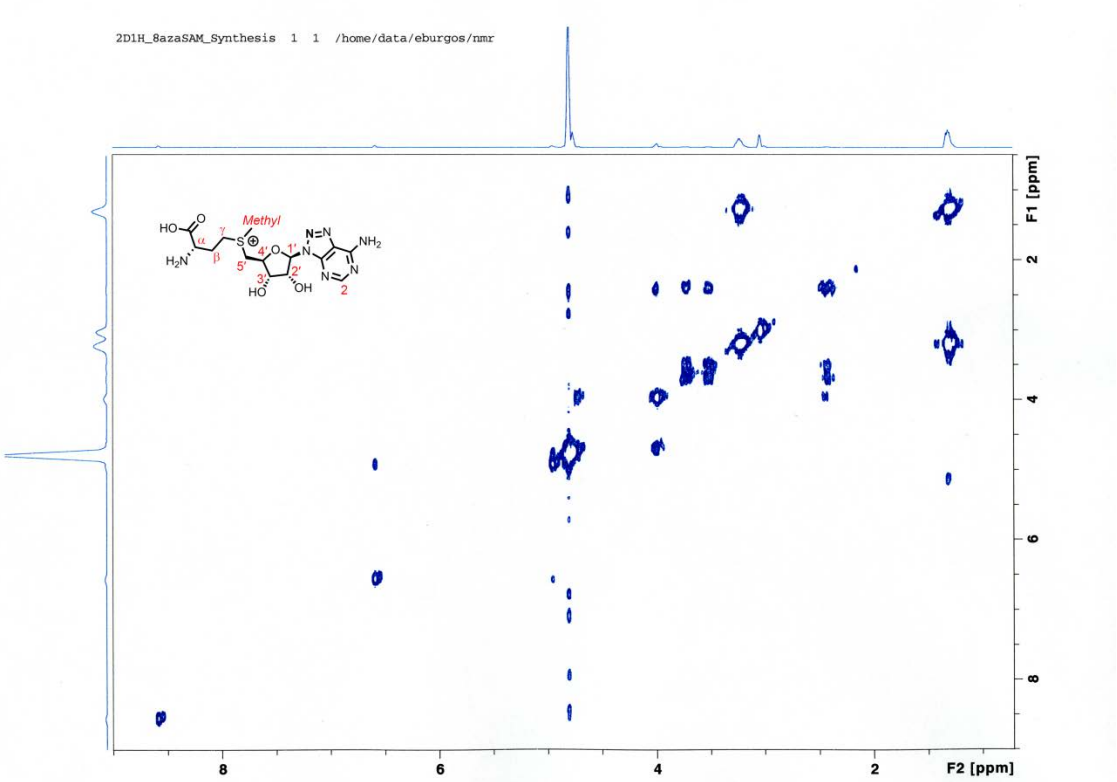
2D1H_8azaSAM_Synthesis 1 1 /home/data/eburgos/nmr
Methyl
F1 [ppm]
F2 [ppm]

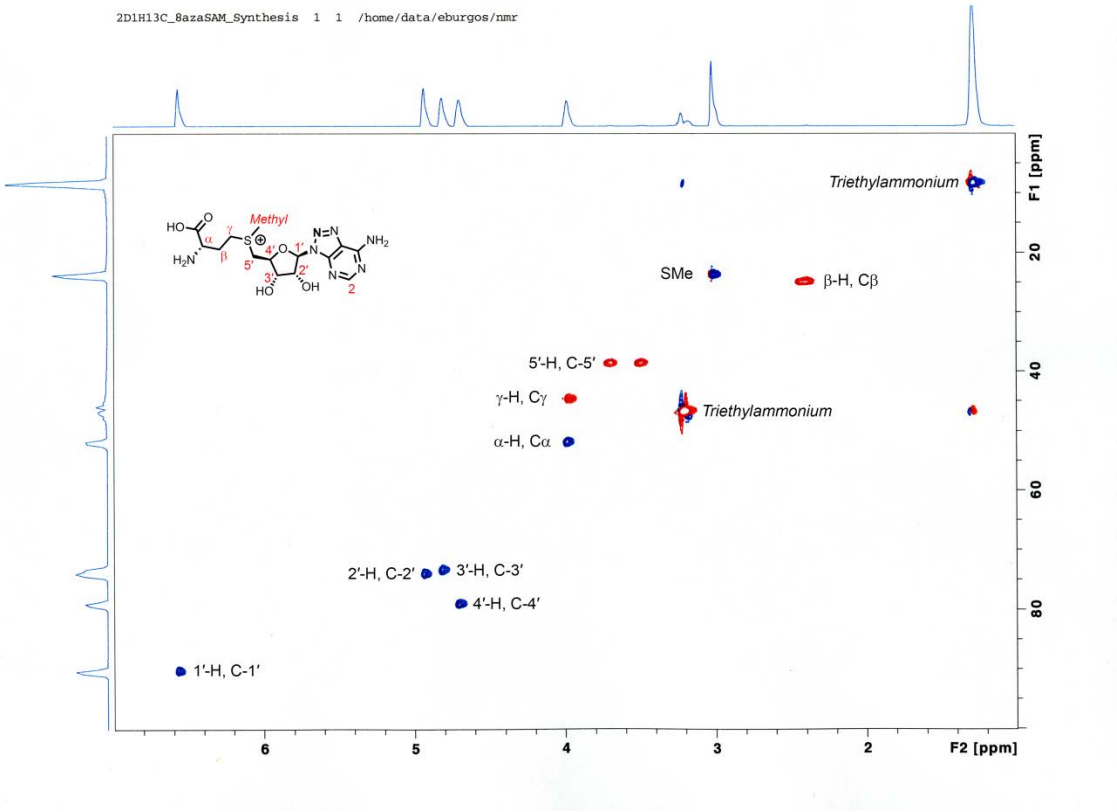
2D1H13C_8azaSAM_Synthesis 1 1 /home/data/eburgos/nmr
Methyl
Triethylammonium
SMe
β-H, Cβ
5′-H, C-5′
γ-H, Cγ
Triethylammonium
α-H, Cα
2′-H, C-2′
3′-H, C-3′
4′-H, C-4′
1′-H, C-1′
F1 [ppm]
F2 [ppm]

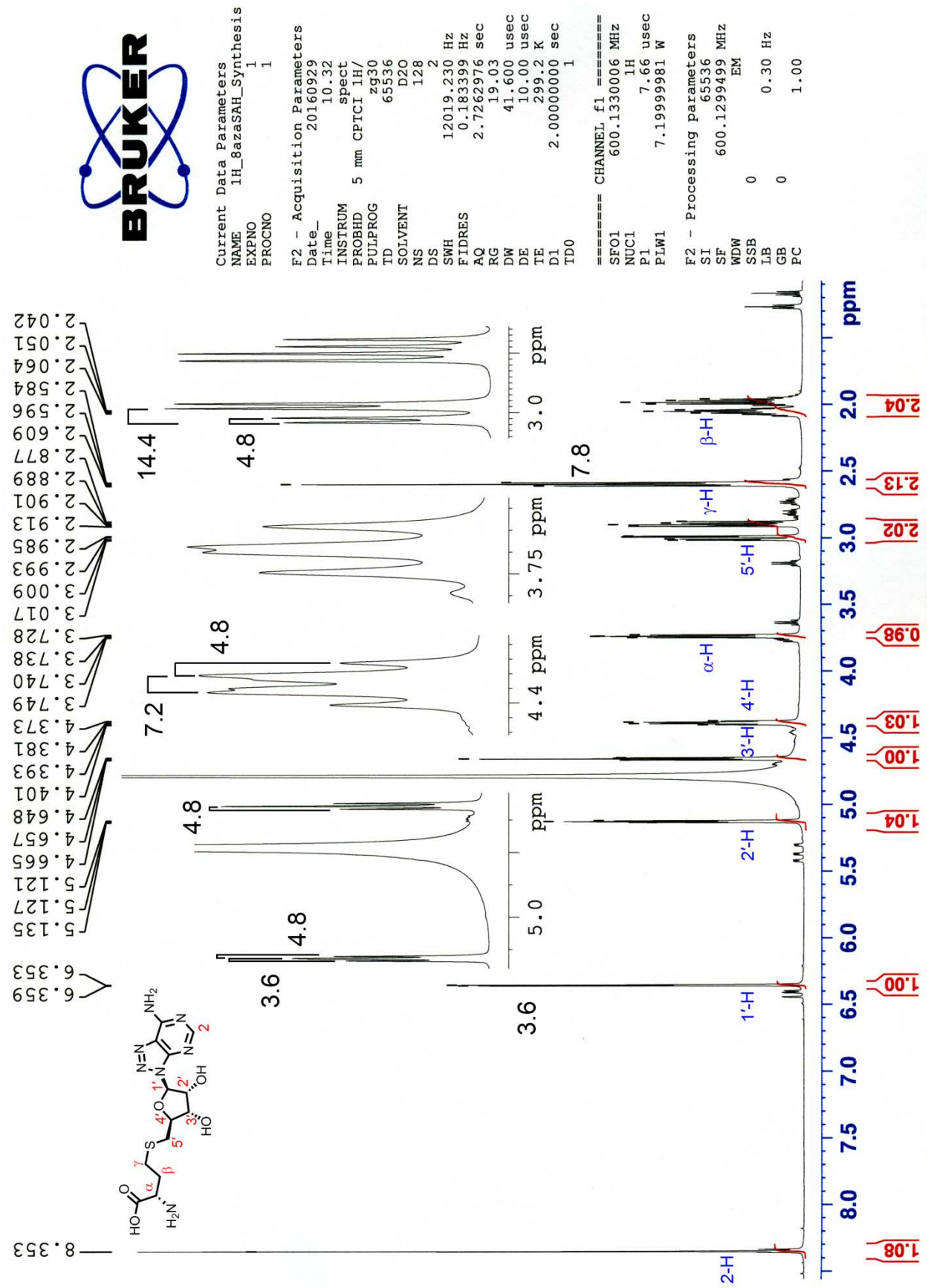
Current Data Parameters
NAME 1H_8azaSAH_Synthesis
EXPNO 1
PROCNO 1
F2 - Acquisition Parameters
Date_ 20160929
Time 10.32
INSTRUM spect
PROBHD 5 mm CPTCI 1H/
PULPROG zg30
TD 65536
SOLVENT D2O
NS 128
DS 2
SWH 12019.230 Hz
FIDRES 0.183399 Hz
AQ 2.7262976 sec
RG 19.03
DW 41.600 usec
DE 10.00 usec
TE 299.2 K
D1 2.00000000 sec
TD0 1
======== CHANNEL f1 ========
SFO1 600.1330006 MHz
NUC1 1H
P1 7.66 usec
PLW1 7.19999981 W
F2 - Processing parameters
SI 65536
SF 600.1299499 MHz
WDW EM
SSB 0
LB 0.30 Hz
GB 0
PC 1.00
ppm
2-H
1'-H
2'-H
3'-H
4'-H
5'-H
α-H
β-H
γ-H

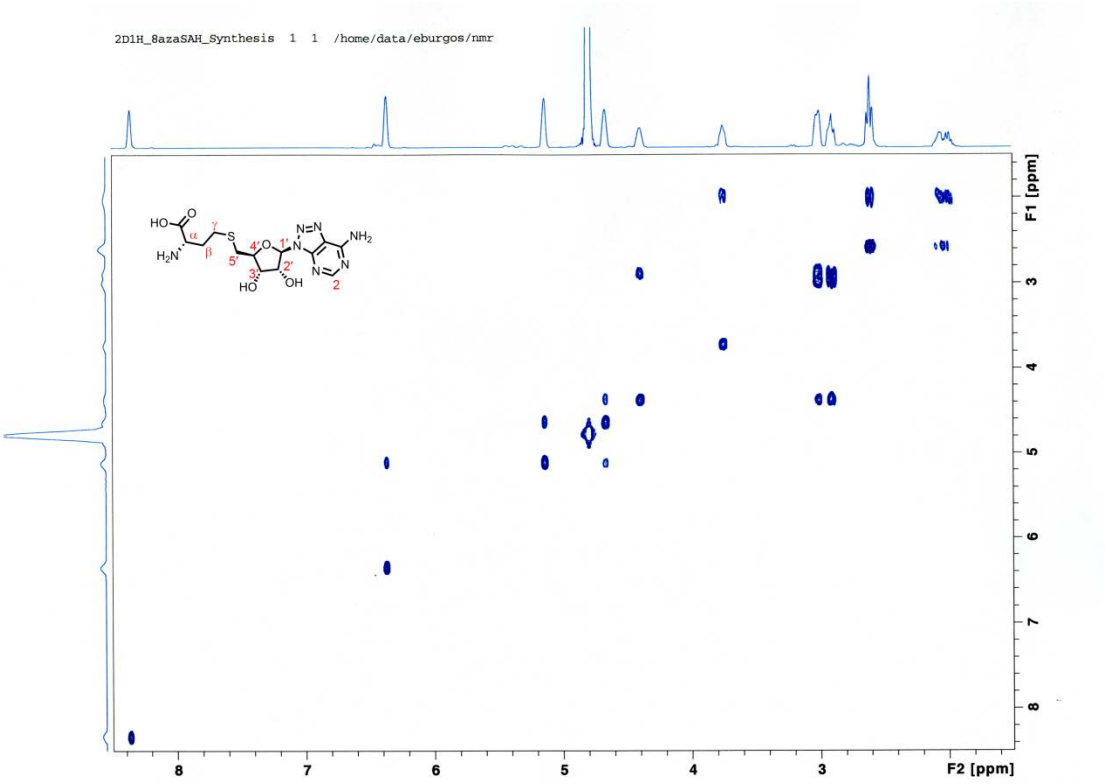
2D1H_8azaSAH_Synthesis 1 1 /home/data/eburgos/nmr
F1 [ppm]
F2 [ppm]

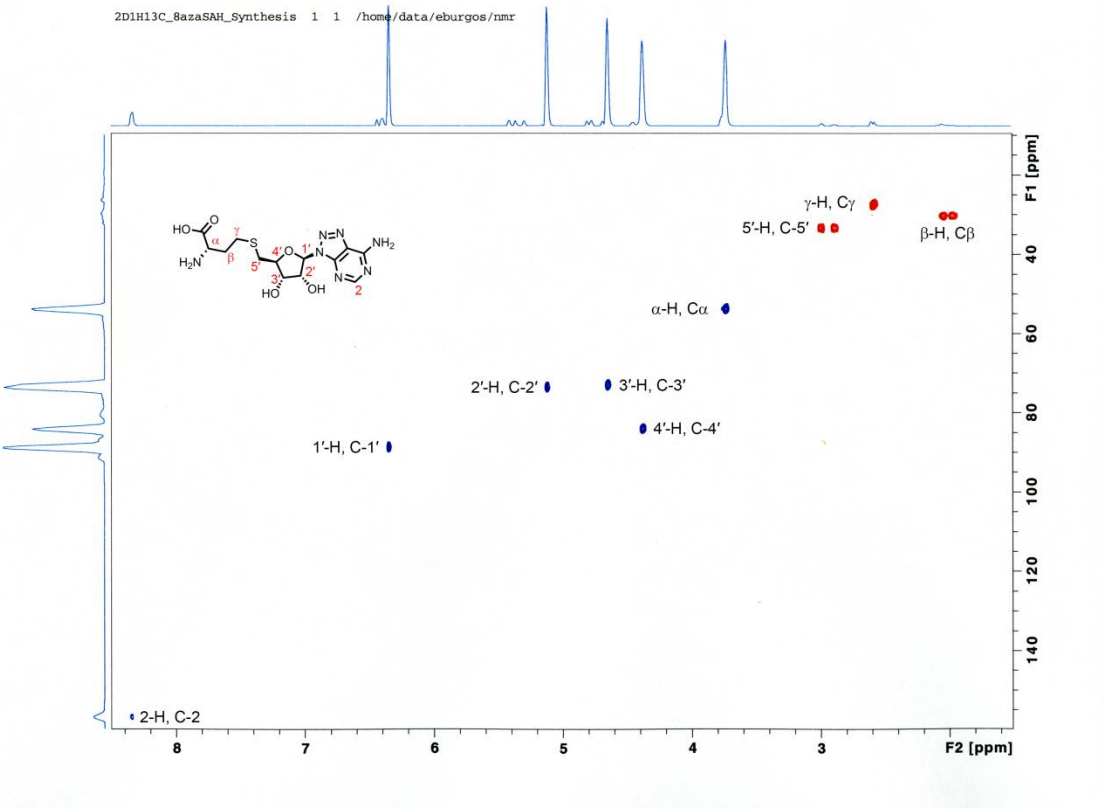
2D1H13C_8azaSAH_Synthesis 1 1 /home/data/eburgos/nmr
γ-H, Cγ
5′-H, C-5′
β-H, Cβ
α-H, Cα
2′-H, C-2′
3′-H, C-3′
4′-H, C-4′
1′-H, C-1′
2-H, C-2
F1 [ppm]
F2 [ppm]

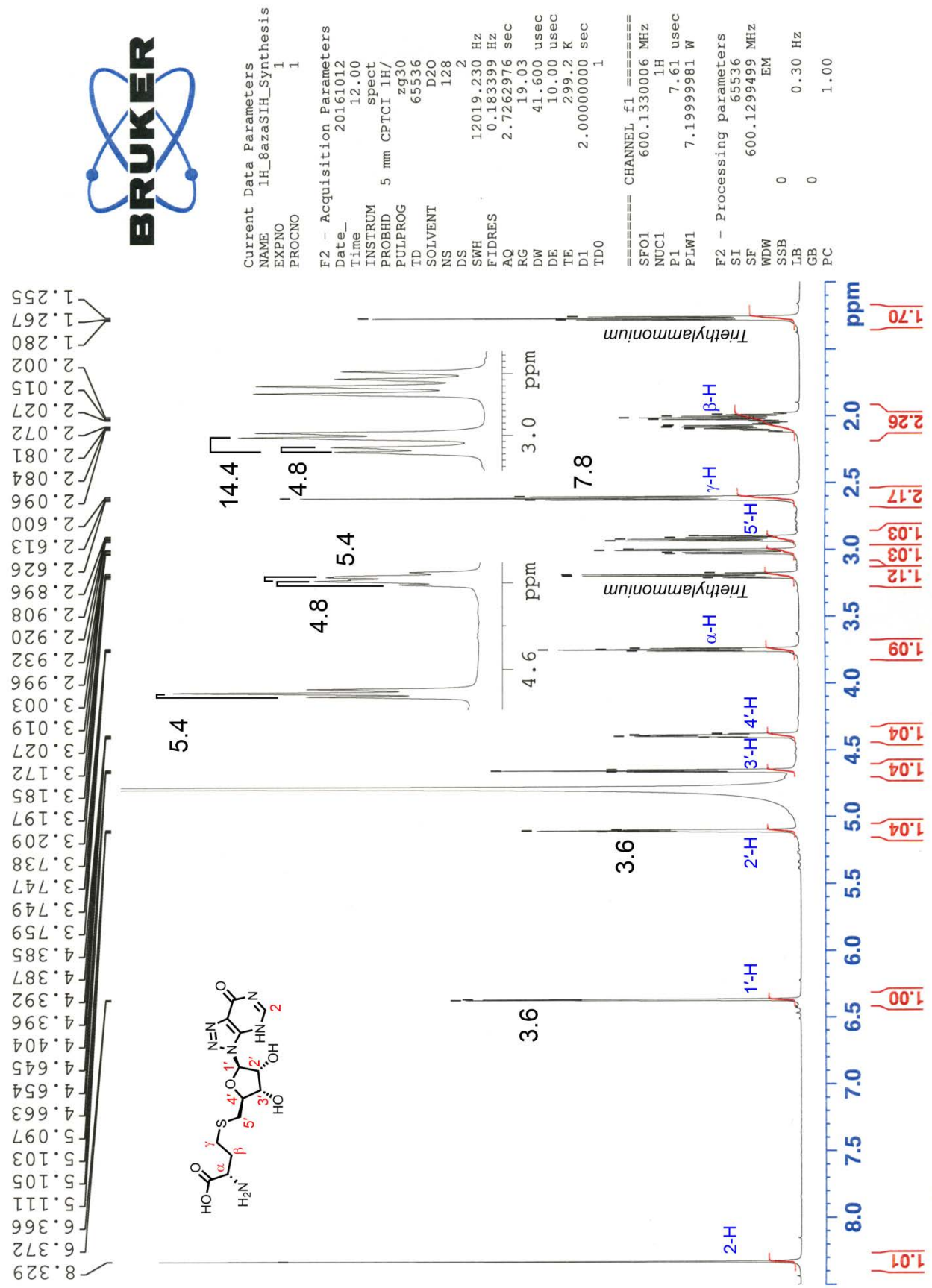
Current Data Parameters
NAME 1H_8azaSIH_Synthesis
EXPNO 1
PROCNO 1
F2 - Acquisition Parameters
Date_ 20161012
Time 12.00
INSTRUM spect
PROBHD 5 mm CPTCI 1H/
PULPROG zg30
TD 65536
SOLVENT D2O
NS 128
DS 2
SWH 12019.230 Hz
FIDRES 0.183399 Hz
AQ 2.7262976 sec
RG 19.03
DW 41.600 usec
DE 10.00 usec
TE 299.2 K
D1 2.00000000 sec
TD0 1
======== CHANNEL f1 ========
SFO1 600.1330006 MHz
NUC1 1H
P1 7.61 usec
PLW1 7.19999981 W
F2 - Processing parameters
SI 65536
SF 600.1299499 MHz
WDW EM
SSB 0
LB 0.30 Hz
GB 0
PC 1.00
Triethylammonium
Triethylammonium
2-H
1'-H
2'-H
3'-H
4'-H
α-H
β-H
γ-H
5'-H
ppm

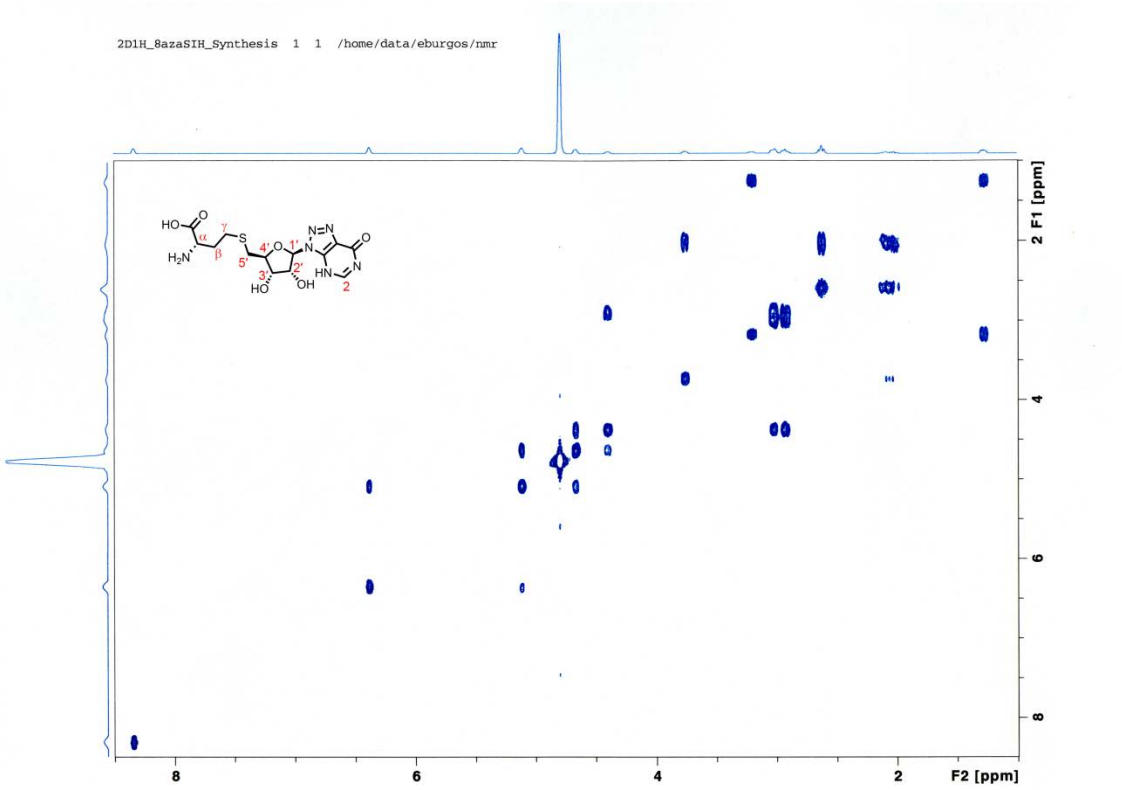
2D1H_8azaSIH_Synthesis 1 1 /home/data/eburgos/nmr
F2 [ppm]
F1 [ppm]

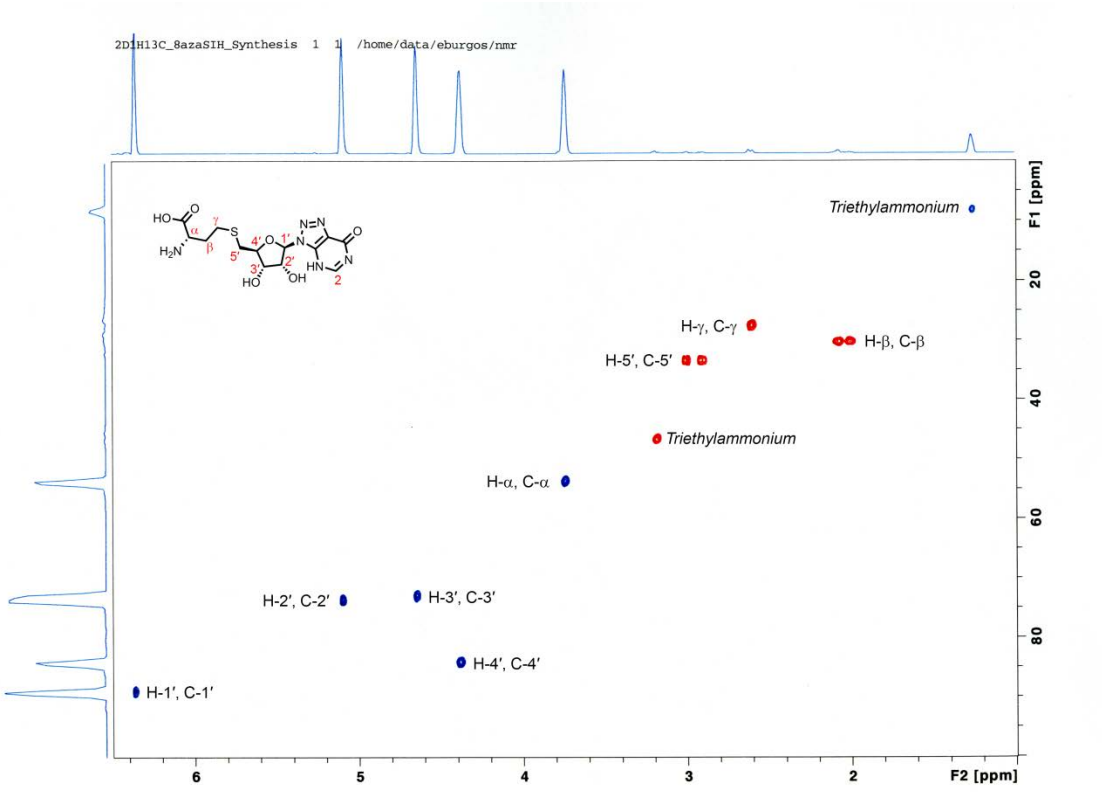
2D1H13C_8azaSIH_Synthesis 1 1 /home/data/eburgos/nmr
Triethylammonium
H-γ, C-γ
H-β, C-β
H-5′, C-5′
Triethylammonium
H-α, C-α
H-2′, C-2′
H-3′, C-3′
H-4′, C-4′
H-1′, C-1′
F2 [ppm]
F1 [ppm]

Supplementary References

1. R. M. McCarty, C. Krebs and V. Bandarian, *Biochemistry*, 2013, **52**, 188-198.
2. B. R. Branchini, M. H. Murtiashaw, R. A. Magyar and S. M. Anderson, *Biochemistry*, 2000, **39**, 5433-5440.
3. M. B. Cassera, M. C. Ho, E. F. Merino, E. S. Burgos, A. Rinaldo-Matthis, S. C. Almo and V. L. Schramm, *Biochemistry*, 2011, **50**, 1885-1893.
4. Z. J. Lu and G. D. Markham, *The Journal of biological chemistry*, 2002, **277**, 16624-16631.
5. F. Garrido, C. Alfonso, J. C. Taylor, G. D. Markham and M. A. Pajares, *Biochimica et biophysica acta*, 2009, **1794**, 1082-1090.
6. J. G. McCoy, L. J. Bailey, Y. H. Ng, C. A. Bingman, R. Wrobel, A. P. Weber, B. G. Fox and G. N. Phillips, Jr., *Proteins*, 2009, **74**, 368-377.
7. L. Sun, M. Wang, Z. Lv, N. Yang, Y. Liu, S. Bao, W. Gong and R. M. Xu, *Proceedings of the National Academy of Sciences of the United States of America*, 2011, **108**, 20538-20543.
8. M. Wang, R. M. Xu and P. R. Thompson, *Biochemistry*, 2013, **52**, 5430-5440.
9. E. W. Debler, K. Jain, R. A. Warmack, Y. Feng, S. G. Clarke, G. Blobel and P. Stavropoulos, *Proceedings of the National Academy of Sciences of the United States of America*, 2016, **113**, 2068-2073.
10. X. Zhang, H. Tamaru, S. I. Khan, J. R. Horton, L. J. Keefe, E. U. Selker and X. Cheng, *Cell*, 2002, **111**, 117-127.
11. E. S. Burgos, C. Wilczek, T. Onikubo, J. B. Bonanno, J. Jansong, U. Reimer and D. Shechter, *The Journal of biological chemistry*, 2015, **290**, 9674-9689.
12. Z. Luka and C. Wagner, *Protein expression and purification*, 2003, **28**, 280-286.
13. J. C. Hermann, R. Marti-Arbona, A. A. Fedorov, E. Fedorov, S. C. Almo, B. K. Shoichet and F. M. Raushel, *Nature*, 2007, **448**, 775-779.
14. A. M. Haapalainen, K. Thomas, P. C. Tyler, G. B. Evans, S. C. Almo and V. L. Schramm, *Structure*, 2013, **21**, 963-974.
15. Y. Wang, H. Akiyama, K. Terakado and T. Nakatsu, *Scientific reports*, 2013, **3**, 2490.
16. G. Cercignani, *Analytical biochemistry*, 1987, **166**, 418-423.
17. J. H. Zhang, T. D. Chung and K. R. Oldenburg, *Journal of biomolecular screening*, 1999, **4**, 67-73.
18. J. F. Morrison, *Biochimica et biophysica acta*, 1969, **185**, 269-286.
19. I. H. Segel, *Enzyme kinetics. Behavior and analysis of rapid equilibrium and steady-state enzyme systems*, John Wiley & Sons, Inc., New York, 1993.
20. D. M. Huffman, G. Farias Quipildor, K. Mao, X. Zhang, J. Wan, P. Apontes, P. Cohen and N. Barzilai, *Aging cell*, 2016, **15**, 181-186.
21. R. J. Cook and C. Wagner, *Proceedings of the National Academy of Sciences of the United States of America*, 1984, **81**, 3631-3634.